Reciprocal Regulation of AMPK-SIRT1 Complex Control of Colorectal Cancer Cell Metastasis by Metformin

Peng Zhou
The Second affiliated hospital of Chongqing medical University
Dan-yang Li
The Second Affiliated Hospital of Chongqing Medical University
Zhu Qiu
The First Affiliated Hospital of Chongqing Medical University
Di Zeng
Chongqing Medical University
Qiang Wei
The First Affiliated Hospital of Chongqing Medical University
Xiao-peng Li
Chongqing Medical University
Jian-hua Ran
Chongqing Medical University
Di-long Chen
Chongqing Medical University
Jing Li (100392@cqmu.edu.cn)
Lab of Stem Cell and Tissue Engineering, Department of Histology and Embryology, Chongqing Medical University, Chongqing 400016, China;

Research

Keywords: colorectal cancer cell, metformin, AMP-activated protein kinase, SIRT1, metastasis

Posted Date: December 15th, 2020

DOI: https://doi.org/10.21203/rs.3.rs-125336/v1

Abstract

Background Liver and lung metastases of Colorectal cancer (CRC) make it as the world's fourth most deadly cancer. AMP-activated protein kinase (AMPK) is a key cellular sensor of metabolism that regulate cellular acetylation levels through distinct mechanisms. However, the acetylation of AMPK and its contribution to regulating CRC metastasis remain poorly understood. This aim of this study was to explore the underlying relationship between AMPK acetylation and CRC metastasis.

Methods

Immunoprecipitation method was used to detected the level of AMPK acetylation in clinical tumor samples and cell samples. Spleen injection model was used to detect the effect of AMPK activator Metformin on liver and lung metastasis. Co-immunoprecipitation, Western blotting, immunofluorescence, and quantitative reverse transcription polymerase chain reaction (RT-qPCR) were conducted to investigate the complex mechanism that reciprocal regulation of AMPK-SIRT1 Complex on CRC metastasis.

Results

In advanced stages of CRC, we observed the increased acetylation of AMPK subunit AMPKβ2. Metformin, an AMPK activator, suppressed the metastasis of HCT-116 cells in the metastasis model. Furthermore, metformin also reduced the migration and invasion of CRC cells *in vitro*. Mechanistic investigation revealed that metformin activated AMPK and induced the deacetylation of AMPKβ2 which was relayed through SIRT1 accumulation. Phosphorylated AMPKα increased the deacetylating activity of SIRT1 by directly phosphorylating SIRT1 at Ser47, and the elevated SIRT1 deacetylated AMPKβ2 to further increase the selective activity of AMPKα on p300 in return. Subsequently, phosphorylated SIRT1 at Ser47 was relocated to the nucleus, and reduced the transcriptional activity of NF-kB/p65 on MMP-9 by deacetylating NF-kB/p65. SIRT1 knockdown or inhibition of AMPK phosphorylation impaired AMPK self-regulatory deacetylation and the anti-metastasis effect of metformin.

Conclusions

Overall, our findings provide new insights into the self-regulatory deacetylation of AMPK in inhibiting CRC metastasis and suggest that metformin has potential therapeutic application against CRC metastasis.

Background

Colorectal cancer (CRC), as the world's fourth most deadly cancer, results in 1.4 million new cases and 0.7 million deaths every year [1]. It is predicted that CRC will dramatically increase by 60% to more than 2.2-million new cases and 1.1 million deaths by 2030 [2]. Despite early detection and therapeutic advances, metastasis, including liver and lung metastases, remains the major cause of death in newly diagnosed CRC patients, and the overall survival of advanced CRC remains unsatisfactory [3]. Thus, novel therapeutic methods or agents need to be developed to improve efficacy against CRC metastasis.

In colon cancer, there are persistent activations of various oncogenic proteins, including NF-κB, β-catenin, and STAT3. Their structural activation leads to tumor proliferation and metastasis, allowing tumor cells to escape apoptosis and generate drug resistance. Taking the NF-κB signaling pathway as an example, NF-κB is essential for regulating the inflammatory process and plays an important role in cell survival, differentiation, proliferation, and migration [4, 5]. Studies have found that dysfunction of NF-κB is closely related to the occurrence and development of colon cancer [6]. The NF-κB family consists of p50 (NF-κB 1), p52 (NF-κB 2), p65 (RelA), c-Rel and RelB, which function as heterodimers and homodimers [7]. When stimulated by conditions such as cytokines, growth factors, and cancer-promoting proteins, NF-κB enters the nucleus from the cytoplasm to promote the transcription of migration and invasion-related proteins MMP-9 and MMP-2 in addition to anti-apoptotic proteins Bcl-2 and Survivin. As the core signal transduction factor of the NF-κB pathway, the transcriptional activity of p65 (RelA) is regulated by its phosphorylation and acetylation status [8]. For example, acetylation of p65 at lysine 221 can significantly enhance its binding to DNA, while acetylation at lysine 310 promotes p65 to achieve full transcriptional activity [9]. In addition, the roles of β-catenin and STAT3 in promoting tumorigenesis are inseparable from their excessive acetylation status.

AMP-activated protein kinase (AMPK) is a key metabolic sensor that can regulate energy homeostasis at the cellular and whole body levels and plays an important role in the coordination of cell growth, metabolism, senescence, migration and invasion [10]. Several studies have shown that activated AMPK may act as a metabolic tumor suppressor by regulating energy levels, enforcing metabolic checkpoints and inhibiting cell growth. There is a vast amount of research demonstrating the tumor suppressor function of AMPK in lung, colorectal, and liver cancers with a growing literature for other cancers, such as prostate and melanoma [11–15]. AMPK consists of a catalytic subunit (α) and two regulatory subunits (β and γ) [16]. The α- and β-subunits both have two isoforms (α1 and α2; β1 and β2), and the γ-subunit has three isoforms (γ1, γ2 and γ3). The α-subunit possesses a transcriptional modification site (Thr172) in the serine/threonine kinase domain responsible for AMPK activity, which is phosphorylated by upstream kinases, such as LKB1 and CaMKKβ [17, 18]. The β-subunit acts as a scaffold to combine the other two subunits [19]. Transcriptional modification of the β-subunit, including phosphorylation, ubiquitination, myristoylation and sumoylation, regulates the activity of AMPK by changing subunit interactions in the enzyme heterotrimer or the cellular location [20, 21]. There are three AMP-binding domains in the γ-subunit, two of which bind AMP or ATP, while the other binds nucleotides [22]. The activation of AMPK involves three complementary mechanisms, including the binding of AMP to the γ-subunit, phosphorylation of the α-subunit (Thr172) by upstream kinases and activity by protein phosphatases (PP2A, PP2C) that leads to the dephosphorylation of the α-subunit (Thr172) [19, 23, 24].

Sirtuins are mammalian homologs of yeast silent information regulator 2 (Sir2) that encodes a histone deacetylase [25]. Among the seven mammalian members of the sirtuins (termed SIRT1-7), SIRT1 shares the greatest identity with yeast Sir2 [26]. As an NAD^+ dependent histone deacetylase, SIRT1 deacetylates histone and non-histone substrates that are involved in a wide variety of cellular functions, particularly in metabolic, oxidative/genotoxic and oncogenic stress responses, including histone H4, histone H3, p53,

FOXO, β-catenin, Ku70, STAT3 and NF-κB [27]. Recent studies have indicated that SIRT1 is overexpressed in many cancer types including liver, breast, prostate and hematopoietic origin, but by activating SIRT1 by natural compounds or overexpression, it also can function as a tumor suppressor [28–31]. The roles and functions of SIRT1 in cancer development have become increasingly complex and are still not well understood.

In recent years, many studies have shown that AMPK and SIRT1 are closely related, and they may function through synergy. On the one hand, SIRT1 can deacetylate AMPK's upstream kinase LKB, leading to phosphorylation of AMPK at Thr172, which activates AMPK [32]. On the other hand, AMPK can promote the expression of Nampt and then upregulate the expression of SIRT1 [33]. It has also been reported that AMPK can form a complex with SIRT1, and phosphorylate SIRT1 at Ser47, and phosphorylation at Ser47 will increase SIRT1 activity[34, 35]. It can be seen that there is a complex regulatory relationship between AMPK and SIRT1, but the specific mechanism needs to be further clarified.

Materials And Methods

Cell culture

Human colorectal cancer cell lines CCD112, HT29, SW480, HCT-116, LOVO and CaCo-2 were purchased form American Type Culture Collection (ATCC) (Manassas, VA, USA). All cell lines were cultured DMEM medium(Gibco, Thermo Fisher Scientific, Inc, Waltham, MA, USA) supplemented with 10% FBS (Thermo Fisher Science, Carlsbad, USA) at 37°C with 5% CO_2. metformin (#HY-B0627, MedChemExpress, Monmouth Junction, NJ, USA) was dissolved in DMEM medium. Sirtnol (HY-13515, MedChemExpress), Lipopolysaccharide (LPS, #HY-D1056, MedChemExpress), TNF-α (#T6674, Sigma, St. Louis, MO, USA) and Compound C (#S7840, Selleck Chemicals, Houston, TX, USA) were dissolved in dimethyl sulfoxide DMSO (#D2650, Sigma, St. Louis, MO, USA).

Wound-closure assay

SW480 cells (5×10^5 cell/well) or HCT-116 cells (3×10^5 cell/well) were plated in 12-well plates for 24 hr and wounded by scratch with a pipette tip. Subsequently, the cells were incubated in complete DEME and treated with or without metformin (0–5 μM) for 24 or 48 hr. Finally, the cells were photographed using a phase-contrast microscope (50 ×).

Transwell Matrigel invasion assay

5×10^5 cell SW480 cells or HCT-116 cells were plated onto a Matrigel (BD Biosciences, Bedford, MA, USA)-coated membrane in the top chamber and incubated for 24 h (24-well insert and 8 μm pore size; Corning Costar, Corning, NY, USA). In this assay, cells pretreated with metformin (0–5 mM) for 1 hr were plated in medium without serum, and medium supplemented with serum was used as a chemoattractant and added to the lower chamber. After 24 hr of incubation, cells that did not invaded through the pores were

removed with a cotton swab. Cells on the lower surface of the membrane were fixed with methanol and stained with crystal violet. The number of cells invading through the membrane was counted under a light microscope (× 200,three random fields per well).

Vascular mimicry (VM) assay

SW480 cells (3×10^4 cell/well), HCT-116 cells (3×10^5 cell/well) or HeLa cells (3×10^5 cell/well) were washed to remove serum, and plated onto a thick (50 μl) layer of a Matrigel (BD Biosciences, Bedford, MA, USA)-coated 96-well plate. In this assay, cells were pretreated with metformin (0–5 mM) for 1 hr, and plated in medium without serum. Cells were imaged 24 h later using a microscope (200 ×) for the presence or absence of networks. All VM experiments were repeated in three independent experiments. Total network length was calculated with the neurite tracing function in the Neuron Growth plug-in ImageJ.

Western blot analysis

Protein lysates were prepared as described previously. A Western blot analysis was performed with primary antibodies specific for MMP-2 (#40994, Cell Signaling Technology, Beverly, MA, USA;1:1000), MMP-9 (#13667), ac-NF-κB/p65 (#12629), NF-κB/p65 (#8242), mTOR (#2983), p-mTOR (Ser2448) (#5536), HDAC1 (#34589), HDAC2 (#57156), HDAC3 (#85057), HDAC4 (#15164), HDAC5 (#20458), HDAC6 (#7558), p300 (#86377), CBP (#7389), SIRT1 (#2493), p-SIRT1 (Ser27) (#2327), p-SIRT1 (Ser47) (#2314), p-AMPK (Ser 172) (#2535), AMPKα (#5832), AMPKβ2 (#4148), acetylated-lysine (#9441), Lamin B1 (#13435), β-actin (#3700), caspase-3 (#SC7272, Santa Cruz Biotechnology, CA, USA). The density of the specific bands was quantified using Image Lab software.

Co-immunoprecipitation

For co-immunoprecipitation experiments, cells were lysed with RIPA buffer [50 mM Tris-HCl (pH 7.2), 150 mM NaCl, 1% (v/v) Triton X-100, 1% (w/v) sodium deoxycholate, 0.1% (w/v) SDS] containing protease inhibitors. Immunoprecipitation was performed by using anti-SIRT1 anti-NF-κB/p65, anti-P300, anti- AMPKα and anti- AMPKβ2 antibodies, and immunocomplexes were analyzed by western blot analysis using the indicated antibodies.

Real-time quantitative PCR

The total RNA was isolated using RNAiso Plus (TaKaRa Biotechnology) according to the manufacturer's instructions. The concentration of RNA was quantified using the NanoDrop 2000c Spectrophotometer (Thermo Fisher Scientific). The first strand cDNA was synthesized from 1 μg of DNase treated total RNA using oligo(dT)18 plus random hexamer primers and M-MLV Reverse Transcriptase (Takara Biotechnology). The qPCR experiments were conducted on Step-One plus real-time PCR System (Applied Biosystems) using SYBR green-I Master PCR Mix with gene specific primers (Supplementary material), and GAPDH was used as reference gene for normalization. The amplifications were performed on three independent samples and triplicate reactions were carried out for each sample. The relative mRNA level was calculated using the $2^{-\Delta\Delta CT}$ method.

Fluorescent staining

Fluorescent staining was performed as described previous[36], and photographed by a fluorescence microscope or a fluorescence confocal microscope.

Knockdown by small interfering RNA

Transfection of the siRNAs was performed using Lipofectamine 2000 (Invitrogen, Carlsbad,

USA) according to the manufacturer's instructions. Small interfering RNAs (siRNA) targeting SIRT1 was purchased from Gene Pharma (Shang Hai, China), and three independent siRNA sequences were used to silence SIRT1 expression.

Sequence 1: sense 5-GCAACUAUACCCAGAACAUTT-3,

antisense 5-AUGUUCUGGGUAUAGUUGCTT – 3V.

Sequence 2: sense 5-GCUGAUGAACCGCUUGCUATT – 3,

antisense 5-UAGCAAGCGGUUCAUCAGCTT – 3V.

Sequence 3: sense 5-GCUGAUGAACCGCUUGCUATT – 3,

antisense 5-UAGCAAGCGGUUCAUCAGCTT – 3V.

In vivo **metastasis model**

Female Balb/c nude mice (4 weeks old) were purchased from the Animal experiment center of Chongqing Medical University and bred in the Animal experiment center. For spleen injection model, luciferase-tagged HCT-116 cells (1×10^6) were suspended in D-Hanks solution and injected into the spleen. After 4 days, the mice were randomized into control and metformin groups according to bioluminescence images taken using IVIS Lumina III (PerkinElmer, Hopkinton, MA, USA). The metformin group was treated with metformin (250 mg/Kg) by gavage (once a day, a total of 28 days), the control group was treated with normal saline. Tumor size and location were monitored every 7 days. For drug combination, the mice were divided into four groups in random: control group, metformin group, capecitabine group (60 mg/Kg, twice weekly by gavage) and combination group. The treatment was followed as described previous. All protocols were reviewed and approved by the Animal experiment center of Chongqing Medical University, and the study was conducted in accordance with the principles of laboratory animal care. After metformin treatment, the mice were sacrificed, tumor specimens were resected, H□E staining and immunohistochemical staining were performed.

Immunohistochemistry and H&E

Patient tissue specimens were analyzed as described previous with anti-SIRT1 antibody, anti-p-SIRT1 antibody and anti-p-AMPK antibody. All tumor specimens were embedded in paraffin blocks and cut into

4-μm sections. Immunostaining and H&E staining were performed according to standard procedures. Immunofluorescent staining for p-AMPKα and p-SIRT1 was performed with specific antibody, followed by anti-rabbit or anti-mouse fluorescent-conjugated antibody and counterstained with the DNA-specific dye Hoechst. A minimum of five randomly selected fields or images were examined in all analyses.

Results

AMPKβ2 acetylation is negatively correlated with AMPKα phosphorylation in advanced stages of CRC

To investigate whether AMPKβ2 can be acetylated, we first investigated the expression of AMPKβ2 acetylation in a panel of CRC cells and one immortalized colon epithelial cell line, CCD 112. Immunoprecipitation revealed that AMPKβ2 could be acetylated and was overexpressed in CRC cell lines compared with CCD 112 cells (Fig. 1a). To further establish the significance of the acetylation level of AMPKβ2, we measured AMPKβ2 expression and acetylation by immunoprecipitation of human colorectal cancer tissues (Fig. 1c, additional file 1: Figure S1a-f). In several non-tumor tissues, the levels of AMPKβ2 acetylation were very low and comparable with normal human colon tissues. By comparison, nearly all tumor tissues had elevated or very elevated levels of AMPKβ2 acetylation. Some non-tumor tissues also displayed elevated AMPKβ2 acetylation, possibly reflecting that these colons are often in a diseased state. Simultaneously, we found the phosphorylation of AMPKα in tumor tissues was significantly reduced compared with the adjacent tissue (Fig. 1b). To analyze the expression of AMPKα phosphorylation in CRC patients, we also used immunohistochemical staining to examine p-AMPK levels in 100 cases of human normal colon tissues and colorectal cancer tissues. The results showed that p-AMPK was highly expressed in normal colon tissues and early stage CRC, and decreased in more advanced stages of CRC (Fig. 1d, e). Interestingly, we found an inverse correlation between AMPKβ2 acetylation and AMPKα phosphorylation in human colorectal cancer tissues as shown in Fig. 1 f. Taken together, these results suggested that the acetylation of AMPKβ2 was negatively correlated with its phosphorylation, while the expression of ac-AMPKβ2 was significantly correlated with CRC malignancy and metastasis.

Anti-metastatic effect of metformin on colon cancer in vivo

To explore the potential relationship between AMPK and tumor metastasis, the AMPK activator metformin was employed to observe the effect of AMPK on metastasis. The anti-migratory and anti-invasive effects of metformin have been demonstrated in various cancer types in vitro [37–39]; however, studies on its anti-metastasis effects in *vivo* are limited. Hence, luciferase-tagged HCT-116 cells were injected into the spleens of Balb/c nude mice. Metformin treatment was initiated four days later. HCT-116-Luc graft mice were administered with vehicle or metformin (250 mg/kg) daily, and tumor metastasis was monitored by a bioluminescence imaging system. In vivo photon emission detection indicated that metformin significantly inhibited the metastasis of colorectal cancer cells during the treatment periods (Fig. 2a, b). After treatment with metformin for two weeks, the luminous intensity of the metastasizing

process was markedly decreased compared with the control group. After treatment (32 days after cell injection) was terminated, mice were sacrificed. The number of visible metastatic lesions was measured. The examination showed that colon cancer metastases developed in the liver, lung and colon of vehicle-treated mice (Fig. 2c-e). Compared with the control group, the metastases were significant inhibited by metformin. These observations revealed that metformin dramatically inhibited metastasis of CRC cells in *vivo.*

Metformin represses CRC growth, migration, invasion and vascular mimicry

Human colorectal cancer cells (SW-480, HCT-116 and CaCo-2) were treated with metformin at different concentrations (0–40 mM) for 24 or 48 h, and the cell viabilities were compared with the control group (Fig. 3a-c). The CCK-8 assay showed that the cell viabilities were significantly reduced by metformin treatment in a time- and dose-dependent manner. In addition, we also used appropriate concentrations of metformin (0–5 mM) to treat CRC cells. No significant changes were observed in the apoptotic marker cleaved caspase-3 between the control and metformin-treated groups (Fig. 3d). These results indicated that metformin treatment (0–5 mM) for 24 h did not inhibit the proliferation of CRC cells. We next studied the effect of metformin on migration and invasion in *vitro*. SW480 and HCT-116 cells were treated with indicated concentrations of metformin in wound closure and Transwell assays for 24 or 48 h, and metformin impaired the performance of CRC cells in both assays concentration-dependently (Fig. 3e-g). In addition, metformin also inhibited the formation of vascular mimicry (Fig. 3h). Overall, we found that metformin remarkably inhibited CRC cell proliferation, migration and invasion.

Metformin activates AMPK and reduces the acetylation of AMPKβ2 in CRC

Studies have shown that AMPK is an important protein involved in sensing and mediating metabolic stress [40]. Moreover, activation of AMPK has been shown to suppress metastasis in many cancers, such as prostate cancer, hepatocellular carcinoma, gastric cancer and colorectal cancer [41–44]. We detected phosphorylated AMPKα, and in metformin-treated cells, the level of p-AMPKα was significantly enhanced in a concentration-dependent manner (Fig. 4a). Downstream of AMPK, mTOR has critical roles in diverse biological processes, such as cell proliferation, survival, autophagy, metabolism, and immunity [45, 46]. We examined the effect of metformin on the activity of mTOR, but the level of p-mTOR was not significantly inhibited by metformin at noncytotoxic concentrations (0–5 mM) (Fig. 4b). To observe the subcellular location of p-AMPK, immunofluorescence staining was performed. In metformin-treated cells, p-AMPK was notably localized to the nucleus(Fig. 4c, d). Studies have shown that p-mTOR is mostly located in the cell cytoplasm and activates substrates related to growth [46, 47]. We speculated that p-AMPK activated by an appropriate concentration of metformin (5 mM) plays a regulatory function in the nucleus. Immunoprecipitation and western blot analysis of treated cells demonstrated that metformin also induced the deacetylation of AMPKβ2 in CRC cells (Fig. 4e). These results indicated that metformin

enhanced the phosphorylation of AMPKα, translocated AMPK from the cytoplasm into the nucleus, and induced the deacetylation of AMPKβ2 in CRC cells.

Metformin inhibits the metastasis of CRC cells through posttranslational modification of NF-κB/p65

Nuclear factor of κB (NF-κB) is a transcription factor with a variety of roles in cell survival, differentiation, proliferation, invasion and migration of cells [48]. It also has been previously shown that NF-κB is constitutively active in CRC tumor cells [49]. We therefore examined the expression levels of several known NF-κB target genes related to cell migration and invasion. The mRNA levels of MMP-9, MMP-2 and ICAM-1 were significantly decreased in CRC cells treated with 5 mM metformin for 1 h (Fig. 5a). Western blot analysis also showed that metformin markedly decreased the expression of MMP-9, a key protein involved in metastasis (Fig. 5b).

The transcriptional activity of NF-κB/p65 is regulated by acetylation at specific sites [50]. To determine if the acetylation NF-κB/p65 was involved in the suppressive role of metformin, we evaluated the acetylation levels of p65 by western blot analysis. The acetylation of NF-κB/p65 was significantly inhibited by metformin, indicating that the suppressive effect on NF-κB/p65 was associated with the anti-metastatic role of metformin (Fig. 5b, c). TNF-α and LPS are important activators of NF-κB and contribute to tumor progression by activating related gene expression [51, 52]. As shown in Fig. 5, TNF-α and LPS caused a substantial increase in the acetylation level of NF-κB/p65 at lysine 310, and the expression of MMP-9 was significantly enhanced (Fig. 5d-f). Metformin thus abolishes constitutive and inducible NF-κB/p65 activation by inhibiting its acetylation. These results indicated that the deacetylation of NF-κB/p65 was involved in the anti-metastatic effect of metformin.

Phosphorylation enhanced the SIRT1 deacetylase activity against NF-κB/p65

To further determine whether metformin lowered acetylation levels in CRC cells, we analyzed whole cell lysates. Western blot analysis using an anti-acetylated-lysine antibody showed that metformin dramatically lowered the whole acetylation level in CRC cells (Fig. 6a). Protein acetylation is controlled by HDACs and HATs [53]. To determine the specific contribution of different classes of HDACs and HATs to the cellular changes induced by metformin, we performed western blotting to inspect related proteins. Among these key HDACs and HATs, HDAC1-HDAC6, SIRT1, CBP and p300 were not observably affected by metformin (Fig. 6b). A previous analysis identified 13 amino acid residues, mainly serine and threonine. as potential SIRT1 phosphorylation sites [54]. We focused on two of these sites (Ser27 and Ser47) that are believed to stabilize the protein or regulate the activity of SIRT1 [34]. Western blot analysis revealed that the total protein level of SIRT1 and the phosphorylation of SIRT1 at Ser27 were not influenced, but metformin significantly enhanced SIRT1 phosphorylation at Ser47 (Fig. 6c-e). We speculated that the phosphorylation may regulate the catalytic activity of SIRT1 toward NF-κB/p65; results showed that metformin altered the SIRT1 deacetylase activity both in SW480 and HCT-116 cells.

To study whether phosphorylation of SIRT1 (Ser47) altered NF-κB/p65 deacetylation after metformin treatment, we performed western blotting on control cells, metformin-induced cells and cells treated with Sirtinol. Compared with the metformin treatment group, Sirtinol significantly increased the expression of ac-NF-κB/p65 and its target protein MMP-9 (Fig. 6f). Altogether, these data indicated that SIRT1 plays a crucial functional role in anti-metastatic effect of metformin on CRC cells.

Metformin suppresses metastasis through AMPK-SIRT1 axis

Previous studies have shown that AMPK can phosphorylate SIRT1 to increase its activity [55, 56]. To further ascertain whether activated AMPK has a biochemical effect in the nucleus, we introduced a directly phosphorylated substrate, p300, to certify the activation of AMPK. Western blot analysis revealed that metformin induced the phosphorylation of AMPKα and upregulated the phosphorylation levels of both SIRT1 and p300. In concurrence, the acetylation level of NF-κB/p65 and the protein level of MMP-9 were decreased in a time-dependent manner (Fig. 7a). Immunoprecipitation of AMPKα from metformin-induced cells followed by western blotting with a specific antibody against p300 confirmed the enhanced formation of the AMPK-p300 complex (Fig. 7b). After Compound C treatment, though the protein level of SIRT1 was not influenced by metformin, but the formation of the AMPK/SIRT1 complex was reduced, with increased expression of ac-NF-κB/p65 (Fig. 7c, d).

We also tested whether the reduced migration and invasion by CRC cells in response to metformin is mediated by the AMPK-SIRT1 signaling pathway. We decided to use Compound C and SIRT1 siRNA to treat CRC cells. The SIRT1 protein was successfully silenced (Fig. 8a). Interestingly, when we used siRNA to silence the expression of SIRT1, the migration and invasion abilities of CRC were significantly elevated (Fig. 8b-e). It is possible that, under normal conditions, SIRT1 can suppress ACOX1 expression by blocking miR-15b-5p transcription to AP-1, which ultimately induces the inhibition of CRC metastasis [31]. Our results showed that both an AMPK inhibitor and SIRT1 siRNA abolished the metformin-induced change in wound closure and the number of invading cells in invasion assays. These results indicate that deacetylation of NF-κB/p65 is mostly dependent on the AMPK-SIRT1 signaling pathway.

Activated AMPK induced by metformin translocates SIRT1 from the cytoplasm into the nucleus

To ascertain the specific mechanism of the regulation of SIRT1 phosphorylation by metformin, we performed fluorescence staining by using an antibody against SIRT1(Ser47). In metformin-induced cells, p-SIRT1 (Ser47) was significantly upregulated and mainly localized in the nuclei of CRC cells (Fig. 9c). The subcellular distribution of SIRT1 was further investigated and quantified by western blot analysis using nuclear and cytoplasmic fractions obtained from CRC cells and metformin-induced cells. Compared with the control group, higher SIRT1 levels were detected in the nuclear fraction after metformin treatment. SIRT1 in the nucleus increased by 220% in SW480 cells and 310% in HCT-116 cells

over a 24 h time period after administration of metformin (Fig. 9a, b). We performed immunofluorescent staining on control cells, metformin-induced cells and cells treated with Compound C. In Compound C-treated cells, the conspicuous nuclear localization of SIRT1 was markedly decreased compared with the metformin group (Fig. 9c). Collectively, these data suggest that AMPK induced SIRT1 translocation to the cell nucleus by regulating the phosphorylation of SIRT1. These findings indicated that AMPKα directly phosphorylated SIRT1 at Ser47, translocated it from the cytoplasm to the nucleus, and that the formation of AMPK/SIRT1 promoted SIRT1 enzymatic activity via phosphorylation.

Self-regulatory deacetylation of AMPK through SIRT1 accumulation; deacetylation of AMPKβ2 elevated its selective activity

To further determine the mechanism of the deacetylation effect of metformin on AMPK, cellular localization of SIRT1 was examined after treatment with metformin. Fluorescence staining demonstrated that SIRT1 was localized both in the cytoplasmic and nuclear compartments in the control group. Treatment with metformin did not increase the SIRT1 protein level but induced the nuclear localization of SIRT1 accompanied with a high level of p-AMPK in the nucleus (Fig. 10a). We analyzed AMPK/SIRT1 complex formation and found that this was upregulated after metformin treatment (Fig. 10b). At the same time, the acetylation level of AMPKβ2 was dramatically decreased. Considering the previous result and the same subcellular localization with SIRT1, we assumed that activated AMPK not only phosphorylated SIRT1 to increase its enzyme activity, but that the accumulation of SIRT1 also induced the deacetylation of AMPKβ2 which increased the activity of AMPK in return. To test our hypothesis, we transfected CRC cells with siRNA against SIRT1. Metformin significantly induced the phosphorylation of AMPKα, and the SIRT1 siRNA had no obvious effect on that phosphorylation (Fig. 10c). This result indicated that AMPK was upstream of SIRT1 in metformin-induced cells. Western blot assays showed that the deacetylation of AMPKβ2 was recovered by SIRT1 siRNA, indicating that SIRT1 was responsible for the deacetylation of AMPKβ2. To determine if acetylation regulates the selective activity of AMPK in the nucleus, we performed western blotting to detect the influence of AMPK on p300 with the silencing of SIRT1. The elevated phosphorylation of p300 induced by AMPK was also decreased (Fig. 10c).

Since SIRT1 was found to be phosphorylated by AMPKα, we determined whether the deacetylation of AMPKβ2 was self-regulated. We used Compound C to treat the CRC cells. As we speculated, although AMPK did not affect the expression of p300 or SIRT1, p-SIRT1 at Ser47 and p-p300 at Ser89 were markedly inhibited by treatment with Compound C, and the deacetylation of AMPKβ2 was reversed (Fig. 10d). Immunoprecipitation also revealed that Compound C in metformin-induced CRC cells caused a decrease in the AMPK/SIRT1 complex (Fig. 10e). These results revealed that AMPK/SIRT1 complex induced the deacetylation of AMPKβ2, and that deacetylation increased the selective activity of AMPK in nucleus.

Metformin activated AMPK/SIRT1 axis in vivo **and synergistically enhances the capecitabine-induced anti-tumor effect**

To determine whether metformin activates the AMPK/SIRT1 axis *in vivo*, samples from the pool of tumor tissues that generated HCT-116 cells were analyzed. Immunofluorescent staining revealed that the phosphorylation levels of AMPKα and SIRT1 (Ser47) were significantly upregulated. Consistent with our previous results, p-SIRT1 was mostly located in the nucleus (Fig. 11a, b). The expressions of p-AMPK and p-SIRT1 (Ser47) were significantly increased in the metformin group. Immunoprecipitation for AMPKβ2 showed that the acetylation of AMPKβ2 was also downregulated (Fig. 11c). These results demonstrated that metformin activated the AMPK-SIRT1 axis *in vivo* to repress the metastasis of CRC.

We also investigated whether metformin in combination with capecitabine inhibited the metastasis of CRC. Treatment was initiated four days after HCT-116 cells were injected into mouse spleens. The treatment lasted for 28 days, then mice were sacrificed and examined for the presence of metastases. metformin alone inhibited metastases to some extent, as did capecitabine in most organs; however, when they were used in combination, the inhibition of metastasis was the highest in these mice (Fig. 11d). Overall, our data suggested that metformin activated the AMPK/SIRT1 axis in *vivo*, and that metformin alone or in combination with capecitabine repressed metastasis in *vivo*.

Discussion

In this study, we found that metformin can inhibit cell survival, invasion and migration *in vitro* and suppress colon cancer metastasis *in vivo*. Mechanistically, metformin strongly induced the phosphorylation of AMPKα at Thr172. Phosphorylated AMPKα increased the deacetylating activity of SIRT1 by directly phosphorylating SIRT1 at Ser47, and the elevated SIRT1 deacetylated AMPKβ2 to further increase the selective activity of AMPKα in return. Subsequently, phosphorylated SIRT1 at Ser47 was relocated to the nucleus and inhibited metastasis by deacetylating NF-κB/p65. Importantly, in support of the results form colon cancer cell lines, studies of clinical specimens showed that the acetylation level of AMPKβ2 was negatively correlated with p-AMPKα(Thr172) and that the acetylation level of AMPKβ2 increased in advanced stages of colon cancer. In summary, we discovered an adjustment function of SIRT1 on the activity of AMPK by deacetylating AMPKβ2, which provides a new avenue for understanding how AMPK inhibits tumor development and progression.

There have been several reports describing how the activation of AMPK can inhibit proliferation and metastasis induced by different stimulants, whereas a decrease in AMPK activity is associated with increased CRC malignancy[57]. A previous study discovered that Sip2(a β-regulatory subunit of yeast AMPK, similar to AMPKβ in humans) acetylation enhances physical interaction with Snf1 (AMPKα) and thereby antagonizes catalytic activity[58]. It has also been reported that phosphorylation of Ser24/25 and Ser182 residues of AMPKβ1, although they do not affect AMPK activity, are necessary for the nuclear exclusion of the β1 subunit, whereas phosphorylation of Ser108, although it does not affect the subcellular distribution of AMPKβ1, increases AMPK activity [20]. Sumoylation of AMPKβ2 enhances the

phosphorylation status of Thr172 in the catalytic subunit and the activity of the AMPK complex, probably because this modification either improves the phosphorylation of AMPK by upstream kinases or prevents the dephosphorylation of AMPK by making it a poorer substrate for specific phosphatases [59]. These reports indicate that AMPKβ subunits are also critical players in AMPK function, because they can regulate the phosphorylation status and subcellular localization of the AMPK complex. Our results revealed that AMPKβ2 can be acetylated and is overexpressed in CRC cell lines compared with CCD 112 cells. We also found an inverse correlation between AMPKβ2 acetylation and AMPKα phosphorylation in human colorectal cancer tissues.

We employed metformin, an activator of AMPK, to further investigate the underlaying relationship between AMPKβ2 acetylation and AMPKα phosphorylation. By analyzing acetyltransferase and deacetylase, we found that phospho-AMPKα regulated AMPKβ2 acetylation by forming an AMPK/SIRT1 complex. SIRT1, an NAD^+ dependent histone deacetylase, was directly phosphorylated by AMPKα at Ser47. A previous study has shown that JNK1, which directly phosphorylates SIRT1 at Ser27, Ser47, and Thr530, concentrates it into the nucleus. In the nucleus, phosphorylated SIRT1 selectively deacetylates histone H3, but not p53[34]. Nin et al. have found that SIRT1 is phosphorylated at Ser47 upon AMPK activation, resulting in an increase in SIRT1 activity; in addition, a low dose of metformin promotes hepatoma cell senescence instead of apoptosis via the activation of AMPK and the inactivation of SIRT1 deacetylase activity on p53 [60]. These data suggest that the regulation of this process is extremely complex. In fact, when SIRT1 was inhibited by siRNA or Sirtinol, in the present study, the regulation of AMPKα on AMPKβ2 acetylation was abolished. Although we observed that this acetylation of AMPKβ2 had no effect on the phosphorylation AMPKα at Thr172, there was a significant effect on the specific substrate selectivity of AMPK. It has been shown that the transcriptional coactivator p300 is a substrate of AMP-kinase, and that phosphorylation of p300 at Ser89 by AMP-kinase dramatically reduces its HAT activity. P300, as an important HAT protein, acetylates many oncogenic proteins to promote tumor growth, such as NF-κB/p65, STAT3 and β-catenin. Although treatment with siSIRT1 or Sirtinol had no effect on the phosphorylation of AMPKα at Ser172, the deacetylation of AMPKβ2 was abolished and the AMPK/p300 complex was destroyed. Our results show that phosphorylation of SIRT1 at Ser47 is crucial for the selective activity of AMPK.

Our results also showed that metformin inhibits the transcriptional activity of NF-κB/p65 by inducing the phosphorylation of SIRT1 at Ser47. In colorectal cancer, constitutively activated NF-κB/p65 contributes to aggressive behaviors and other malignancies [61]. As the core signaling transducer of the NF-κB pathway, NF-κB/p65 is regulated flexibly with respect to the status of its posttranslational modifications, including phosphorylation and acetylation[8]. Acetylation at distinct lysine residues affects NF-κB activity differently. For instance, lysine 221 acetylation of NF-κB/p65 selectively enhances its DNA binding while lysine 310 acetylation facilitates its full transcriptional activity independent of the regulation of DNA binding or IκBα binding. One study indicates that SIRT1 associates directly with NF-κB/p65 and deacetylates it at lysine 310 to suppresses its transcriptional activity; the blockade of TNFα-induced NF-κB transcription correlates with sensitization of NSCLC cells to TNFα-induced apoptosis. In our study,

phosphorylated SIRT1 was relocated into the nucleus by AMPK, which increased the deacetylation activity of SIRT1 to NF-κB/p65. In fact, inactivated p300 may also be involved in the inhibition effect of AMPK on the transcriptional activity of NF-κB/p65. P300 can influence the acetylation state of NF-κB/p65 by its HAT activity, and phosphorylation of p300 at Ser89 by AMP-kinase dramatically represses the transcriptional activity of NF-κB/p65 on Lys221 and reduces the DNA binding activity of NF-κB/p65 by inhibiting its recruitment to its target gene promoters [62].

Conclusions

In summary, this work enhances our understanding of the reciprocal mechanisms of the AMPK/SIRT1 axis and demonstrates that metformin inhibits tumor metastasis by regulating NF-κB/p65.

Abbreviations

AMPK
AMP-activated protein kinase ;
CRC
Colorectal cancer;
STAT3
Signal Transducer And Activator Of Transcription 3;
Sir2
silent information regulator 2;
VM
Vascular mimicry;
MMP
matrix metalloproteinase;
qRT-PCR
Real-Time Quantitative Reverse Transcription PCR

Declarations

Ethics approval and consent to participate

The human cancer tissues used in this study were approved by the institute. Ethical committee of Chongqing **Medical University. All patients gave written informed consent.**

Consent for publication

The consent forms were signed by every participant and will be provided upon request.

Availability of data and materials

The datasets used and/or analyzed during the current study were available **from the corresponding authors on reasonable request.**

Competing interests

Authors declare that there is no conflict interest.

Funding

This work was supported by the National Natural Science Foundation of China (Grant No. 81803110).

Authors' contributions

PZ was responsible for ***in*** *vivo* metastasis model**,** *in vitro* cell operation**,** and first **manuscript draft.** Dan-yang Li **performed cell transfection** and cell and tissue staining**.ZQ** collect**edtissue**. DZ helped us with wound-closure, transwell and Vascular mimicry assay. **Q**W and XPL **analyzed the data and data validation**. JL **contributed to study design and final manuscript approval.** JHR and DLC **helped us with the study design**. **All authors read and approved the final manuscript.**

Acknowledgements

We thank LetPub (www.letpub.com) for its linguistic assistance during the preparation of this

Manuscript.

Authors' information

Peng Zhou, Email: zp979391906@163.com

Dan-yang Li , Email: lidycq@cqmu.edu.cn

Zhu Qiu, Email: qiuzhu523@163.com

Di Zeng , Email: 707194568@qq.com

Qiang Wei, Email: 1047890186@qq.com

Xiao-peng Li , Email: lxp19890204@163.com

Jian-hua Ran, Email: ranjianhua@cqmu.edu.cn

Di-long Chen, Email: xinmengyuandlc@163.com

Jing Li, Email: 100392@cqmu.edu.cn

References

[1] H. Brody, Colorectal cancer, Nature, 521 (2015) S1.

[2] M. Arnold, M.S. Sierra, M. Laversanne, I. Soerjomataram, A. Jemal, F. Bray, Global patterns and trends in colorectal cancer incidence and mortality, Gut, 66 (2017) 683-691.

[3] D. Huang, W. Sun, Y. Zhou, P. Li, F. Chen, H. Chen, D. Xia, E. Xu, M. Lai, Y. Wu, H. Zhang, Mutations of key driver genes in colorectal cancer progression and metastasis, Cancer Metastasis Rev, 37 (2018) 173-187.

[4] M. Karin, M. Delhase, The I kappa B kinase (IKK) and NF-kappa B: key elements of proinflammatory signalling, Semin Immunol, 12 (2000) 85-98.

[5] J.L. Luo, H. Kamata, M. Karin, The anti-death machinery in IKK/NF-kappaB signaling, J Clin Immunol, 25 (2005) 541-550.

[6] M. Karin, Nuclear factor-kappaB in cancer development and progression, Nature, 441 (2006) 431-436.

[7] M.C. Arkan, F.R. Greten, IKK- and NF-kappaB-mediated functions in carcinogenesis, Curr Top Microbiol Immunol, 349 (2011) 159-169.

[8] N.D. Perkins, Post-translational modifications regulating the activity and function of the nuclear factor kappa B pathway, Oncogene, 25 (2006) 6717-6730.

[9] W.C. Greene, L.F. Chen, Regulation of NF-kappaB action by reversible acetylation, Novartis Found Symp, 259 (2004) 208-217; discussion 218-225.

[10] M.K. Pandey, S.C. Gupta, A. Nabavizadeh, B.B. Aggarwal, Regulation of cell signaling pathways by dietary agents for cancer prevention and treatment, Semin Cancer Biol, 46 (2017) 158-181.

[11] L. Ding, G. Getz, D.A. Wheeler, E.R. Mardis, M.D. McLellan, K. Cibulskis, C. Sougnez, H. Greulich, D.M. Muzny, M.B. Morgan, L. Fulton, R.S. Fulton, Q. Zhang, M.C. Wendl, M.S. Lawrence, D.E. Larson, K. Chen, D.J. Dooling, A. Sabo, A.C. Hawes, H. Shen, S.N. Jhangiani, L.R. Lewis, O. Hall, Y. Zhu, T. Mathew, Y. Ren, J. Yao, S.E. Scherer, K. Clerc, G.A. Metcalf, B. Ng, A. Milosavljevic, M.L. Gonzalez-Garay, J.R. Osborne, R. Meyer, X. Shi, Y. Tang, D.C. Koboldt, L. Lin, R. Abbott, T.L. Miner, C. Pohl, G. Fewell, C. Haipek, H. Schmidt, B.H. Dunford-Shore, A. Kraja, S.D. Crosby, C.S. Sawyer, T. Vickery, S. Sander, J. Robinson, W. Winckler, J. Baldwin, L.R. Chirieac, A. Dutt, T. Fennell, M. Hanna, B.E. Johnson, R.C. Onofrio, R.K. Thomas, G. Tonon, B.A. Weir, X. Zhao, L. Ziaugra, M.C. Zody, T. Giordano, M.B. Orringer, J.A. Roth, M.R. Spitz, Wistuba, II, B. Ozenberger, P.J. Good, A.C. Chang, D.G. Beer, M.A. Watson, M. Ladanyi, S. Broderick, A. Yoshizawa, W.D. Travis, W. Pao, M.A. Province, G.M. Weinstock, H.E. Varmus, S.B. Gabriel, E.S. Lander, R.A. Gibbs, M. Meyerson, R.K. Wilson, Somatic mutations affect key pathways in lung adenocarcinoma, Nature, 455 (2008) 1069-1075.

[12] Y. Baba, K. Nosho, K. Shima, J.A. Meyerhardt, A.T. Chan, J.A. Engelman, L.C. Cantley, M. Loda, E. Giovannucci, C.S. Fuchs, S. Ogino, Prognostic significance of AMP-activated protein kinase expression

and modifying effect of MAPK3/1 in colorectal cancer, Br J Cancer, 103 (2010) 1025-1033.

[13] L. Zheng, W. Yang, F. Wu, C. Wang, L. Yu, L. Tang, B. Qiu, Y. Li, L. Guo, M. Wu, G. Feng, D. Zou, H. Wang, Prognostic significance of AMPK activation and therapeutic effects of metformin in hepatocellular carcinoma, Clin Cancer Res, 19 (2013) 5372-5380.

[14] R.R. Chhipa, Y. Wu, C. Ip, AMPK-mediated autophagy is a survival mechanism in androgen-dependent prostate cancer cells subjected to androgen deprivation and hypoxia, Cell Signal, 23 (2011) 1466-1472.

[15] H.S. Kim, M.J. Kim, E.J. Kim, Y. Yang, M.S. Lee, J.S. Lim, Berberine-induced AMPK activation inhibits the metastatic potential of melanoma cells via reduction of ERK activity and COX-2 protein expression, Biochem Pharmacol, 83 (2012) 385-394.

[16] A.S. Kim, E.J. Miller, L.H. Young, AMP-activated protein kinase: a core signalling pathway in the heart, Acta Physiol (Oxf), 196 (2009) 37-53.

[17] G.R. Steinberg, D. Carling, AMP-activated protein kinase: the current landscape for drug development, Nat Rev Drug Discov, 18 (2019) 527-551.

[18] K.L. Marcelo, A.R. Means, B. York, The Ca(2+)/Calmodulin/CaMKK2 Axis: Nature's Metabolic CaMshaft, Trends Endocrinol Metab, 27 (2016) 706-718.

[19] P. Sanz, T. Rubio, M.A. Garcia-Gimeno, AMPKbeta subunits: more than just a scaffold in the formation of AMPK complex, FEBS J, 280 (2013) 3723-3733.

[20] S.M. Warden, C. Richardson, J. O'Donnell, Jr., D. Stapleton, B.E. Kemp, L.A. Witters, Post-translational modifications of the beta-1 subunit of AMP-activated protein kinase affect enzyme activity and cellular localization, Biochem J, 354 (2001) 275-283.

[21] D. Moreno, M.C. Towler, D.G. Hardie, E. Knecht, P. Sanz, The laforin-malin complex, involved in Lafora disease, promotes the incorporation of K63-linked ubiquitin chains into AMP-activated protein kinase beta subunits, Mol Biol Cell, 21 (2010) 2578-2588.

[22] D.G. Hardie, D. Carling, S.J. Gamblin, AMP-activated protein kinase: also regulated by ADP?, Trends Biochem Sci, 36 (2011) 470-477.

[23] S.C. Lin, D.G. Hardie, AMPK: Sensing Glucose as well as Cellular Energy Status, Cell Metab, 27 (2018) 299-313.

[24] S.P. Davies, N.R. Helps, P.T. Cohen, D.G. Hardie, 5'-AMP inhibits dephosphorylation, as well as promoting phosphorylation, of the AMP-activated protein kinase. Studies using bacterially expressed human protein phosphatase-2C alpha and native bovine protein phosphatase-2AC, FEBS Lett, 377 (1995) 421-425.

[25] S. Imai, C.M. Armstrong, M. Kaeberlein, L. Guarente, Transcriptional silencing and longevity protein Sir2 is an NAD-dependent histone deacetylase, Nature, 403 (2000) 795-800.

[26] S. Michan, D. Sinclair, Sirtuins in mammals: insights into their biological function, Biochem J, 404 (2007) 1-13.

[27] M. Roth, W.Y. Chen, Sorting out functions of sirtuins in cancer, Oncogene, 33 (2014) 1609-1620.

[28] I.C. Chen, W.F. Chiang, H.H. Huang, P.F. Chen, Y.Y. Shen, H.C. Chiang, Role of SIRT1 in regulation of epithelial-to-mesenchymal transition in oral squamous cell carcinoma metastasis, Mol Cancer, 13 (2014) 254.

[29] L.F. Costa-Machado, R. Martin-Hernandez, M.A. Sanchez-Luengo, K. Hess, C. Vales-Villamarin, M. Barradas, C. Lynch, D. de la Nava, A. Diaz-Ruiz, R. de Cabo, M. Canamero, L. Martinez, M. Sanchez-Carbayo, D. Herranz, M. Serrano, P.J. Fernandez-Marcos, Sirt1 protects from K-Ras-driven lung carcinogenesis, EMBO Rep, 19 (2018).

[30] L. Sun, H. Li, J. Chen, V. Dehennaut, Y. Zhao, Y. Yang, Y. Iwasaki, B. Kahn-Perles, D. Leprince, Q. Chen, A. Shen, Y. Xu, A SUMOylation-dependent pathway regulates SIRT1 transcription and lung cancer metastasis, J Natl Cancer Inst, 105 (2013) 887-898.

[31] L.N. Sun, Z. Zhi, L.Y. Chen, Q. Zhou, X.M. Li, W.J. Gan, S. Chen, M. Yang, Y. Liu, T. Shen, Y. Xu, J.M. Li, SIRT1 suppresses colorectal cancer metastasis by transcriptional repression of miR-15b-5p, Cancer Lett, 409 (2017) 104-115.

[32] S. Wang, Y. Wang, Z. Zhang, Q. Liu, J. Gu, Cardioprotective effects of fibroblast growth factor 21 against doxorubicin-induced toxicity via the SIRT1/LKB1/AMPK pathway, Cell Death Dis, 8 (2017) e3018.

[33] M. Fulco, Y. Cen, P. Zhao, E.P. Hoffman, M.W. McBurney, A.A. Sauve, V. Sartorelli, Glucose restriction inhibits skeletal myoblast differentiation by activating SIRT1 through AMPK-mediated regulation of Nampt, Dev Cell, 14 (2008) 661-673.

[34] N. Nasrin, V.K. Kaushik, E. Fortier, D. Wall, K.J. Pearson, R. de Cabo, L. Bordone, JNK1 phosphorylates SIRT1 and promotes its enzymatic activity, PLoS One, 4 (2009) e8414.

[35] Z.Y. Zhang, D. Hong, S.H. Nam, J.M. Kim, Y.H. Paik, J.W. Joh, C.H. Kwon, J.B. Park, G.S. Choi, K.Y. Jang, C.K. Park, S.J. Kim, SIRT1 regulates oncogenesis via a mutant p53-dependent pathway in hepatocellular carcinoma, J Hepatol, 62 (2015) 121-130.

[36] D. Li, A. Chen, T. Lan, Y. Zou, L. Zhao, P. Yang, H. Qu, L. Wei, Z. Varghese, J.F. Moorhead, Y. Chen, X.Z. Ruan, SCAP knockdown in vascular smooth muscle cells alleviates atherosclerosis plaque formation via up-regulating autophagy in ApoE(-/-) mice, FASEB J, 33 (2019) 3437-3450.

[37] X. Bao, L. Zhao, H. Guan, F. Li, Inhibition of LCMR1 and ATG12 by demethylation-activated miR-570-3p is involved in the anti-metastasis effects of metformin on human osteosarcoma, Cell Death Dis, 9 (2018) 611.

[38] L. Song, J. Guo, R. Chang, X. Peng, J. Li, X. Xu, X. Zhan, L. Zhan, LKB1 obliterates Snail stability and inhibits pancreatic cancer metastasis in response to metformin treatment, Cancer Sci, 109 (2018) 1382-1392.

[39] M. Tyszka-Czochara, M. Lasota, M. Majka, Caffeic Acid and Metformin Inhibit Invasive Phenotype Induced by TGF-beta1 in C-4I and HTB-35/SiHa Human Cervical Squamous Carcinoma Cells by Acting on Different Molecular Targets, Int J Mol Sci, 19 (2018).

[40] J. Tsalikis, D.O. Croitoru, D.J. Philpott, S.E. Girardin, Nutrient sensing and metabolic stress pathways in innate immunity, Cell Microbiol, 15 (2013) 1632-1641.

[41] X. Jiang, H.Y. Tan, S. Teng, Y.T. Chan, D. Wang, N. Wang, The Role of AMP-Activated Protein Kinase as a Potential Target of Treatment of Hepatocellular Carcinoma, Cancers (Basel), 11 (2019).

[42] C.C. Su, K.L. Hsieh, P.L. Liu, H.C. Yeh, S.P. Huang, S.H. Fang, W.C. Cheng, K.H. Huang, F.Y. Chiu, I.L. Lin, M.Y. Huang, C.Y. Li, AICAR Induces Apoptosis and Inhibits Migration and Invasion in Prostate Cancer Cells Through an AMPK/mTOR-Dependent Pathway, Int J Mol Sci, 20 (2019).

[43] Y. Yao, X. Yang, L. Sun, S. Sun, X. Huang, D. Zhou, T. Li, W. Zhang, N.A. Abumrad, X. Zhu, S. He, X. Su, Fatty acid 2-hydroxylation inhibits tumor growth and increases sensitivity to cisplatin in gastric cancer, EBioMedicine, 41 (2019) 256-267.

[44] Y.H. Han, J.Y. Kee, S.H. Hong, Rosmarinic Acid Activates AMPK to Inhibit Metastasis of Colorectal Cancer, Front Pharmacol, 9 (2018) 68.

[45] F.C. Harwood, R.I. Klein Geltink, B.P. O'Hara, M. Cardone, L. Janke, D. Finkelstein, I. Entin, L. Paul, P.J. Houghton, G.C. Grosveld, ETV7 is an essential component of a rapamycin-insensitive mTOR complex in cancer, Sci Adv, 4 (2018) eaar3938.

[46] R.A. Saxton, D.M. Sabatini, mTOR Signaling in Growth, Metabolism, and Disease, Cell, 168 (2017) 960-976.

[47] N. Schafer, G.H. Gielen, L. Rauschenbach, S. Kebir, A. Till, R. Reinartz, M. Simon, P. Niehusmann, C. Kleinschnitz, U. Herrlinger, T. Pietsch, B. Scheffler, M. Glas, Longitudinal heterogeneity in glioblastoma: moving targets in recurrent versus primary tumors, J Transl Med, 17 (2019) 96.

[48] D. Kabacaoglu, D.A. Ruess, J. Ai, H. Algul, NF-kappaB/Rel Transcription Factors in Pancreatic Cancer: Focusing on RelA, c-Rel, and RelB, Cancers (Basel), 11 (2019).

[49] K. Sakamoto, S. Maeda, Y. Hikiba, H. Nakagawa, Y. Hayakawa, W. Shibata, A. Yanai, K. Ogura, M. Omata, Constitutive NF-kappaB activation in colorectal carcinoma plays a key role in angiogenesis, promoting tumor growth, Clin Cancer Res, 15 (2009) 2248-2258.

[50] J.W. Kim, S.M. Jang, C.H. Kim, J.H. An, E.J. Kang, K.H. Choi, New molecular bridge between RelA/p65 and NF-kappaB target genes via histone acetyltransferase TIP60 cofactor, J Biol Chem, 287 (2012) 7780-7791.

[51] H. Li, J.Q. Xia, F.S. Zhu, Z.H. Xi, C.Y. Pan, L.M. Gu, Y.Z. Tian, LPS promotes the expression of PD-L1 in gastric cancer cells through NF-kappaB activation, J Cell Biochem, 119 (2018) 9997-10004.

[52] Y. Gao, Y. Yang, F. Yuan, J. Huang, W. Xu, B. Mao, Z. Yuan, W. Bi, TNFalpha-YAP/p65-HK2 axis mediates breast cancer cell migration, Oncogenesis, 6 (2017) e383.

[53] J.Y. Fang, Histone deacetylase inhibitors, anticancerous mechanism and therapy for gastrointestinal cancers, J Gastroenterol Hepatol, 20 (2005) 988-994.

[54] T. Sasaki, B. Maier, K.D. Koclega, M. Chruszcz, W. Gluba, P.T. Stukenberg, W. Minor, H. Scrable, Phosphorylation regulates SIRT1 function, PLoS One, 3 (2008) e4020.

[55] B. Xue, Z. Yang, X. Wang, H. Shi, Omega-3 polyunsaturated fatty acids antagonize macrophage inflammation via activation of AMPK/SIRT1 pathway, PLoS One, 7 (2012) e45990.

[56] B. Parodi, S. Rossi, S. Morando, C. Cordano, A. Bragoni, C. Motta, C. Usai, B.T. Wipke, R.H. Scannevin, G.L. Mancardi, D. Centonze, N. Kerlero de Rosbo, A. Uccelli, Fumarates modulate microglia activation through a novel HCAR2 signaling pathway and rescue synaptic dysregulation in inflamed CNS, Acta Neuropathol, 130 (2015) 279-295.

[57] B. Faubert, E.E. Vincent, M.C. Poffenberger, R.G. Jones, The AMP-activated protein kinase (AMPK) and cancer: many faces of a metabolic regulator, Cancer Lett, 356 (2015) 165-170.

[58] J.Y. Lu, Y.Y. Lin, J.C. Sheu, J.T. Wu, F.J. Lee, Y. Chen, M.I. Lin, F.T. Chiang, T.Y. Tai, S.L. Berger, Y. Zhao, K.S. Tsai, H. Zhu, L.M. Chuang, J.D. Boeke, Acetylation of yeast AMPK controls intrinsic aging independently of caloric restriction, Cell, 146 (2011) 969-979.

[59] T. Rubio, S. Vernia, P. Sanz, Sumoylation of AMPKbeta2 subunit enhances AMP-activated protein kinase activity, Mol Biol Cell, 24 (2013) 1801-1811, S1801-1804.

[60] V. Nin, C. Escande, C.C. Chini, S. Giri, J. Camacho-Pereira, J. Matalonga, Z. Lou, E.N. Chini, Role of deleted in breast cancer 1 (DBC1) protein in SIRT1 deacetylase activation induced by protein kinase A and AMP-activated protein kinase, J Biol Chem, 287 (2012) 23489-23501.

[61] T. Cooks, I.S. Pateras, O. Tarcic, H. Solomon, A.J. Schetter, S. Wilder, G. Lozano, E. Pikarsky, T. Forshew, N. Rosenfeld, N. Harpaz, S. Itzkowitz, C.C. Harris, V. Rotter, V.G. Gorgoulis, M. Oren, Mutant p53

prolongs NF-kappaB activation and promotes chronic inflammation and inflammation-associated colorectal cancer, Cancer Cell, 23 (2013) 634-646.

[62] Y. Zhang, J. Qiu, X. Wang, Y. Zhang, M. Xia, AMP-activated protein kinase suppresses endothelial cell inflammation through phosphorylation of transcriptional coactivator p300, Arterioscler Thromb Vasc Biol, 31 (2011) 2897-2908.

Figures

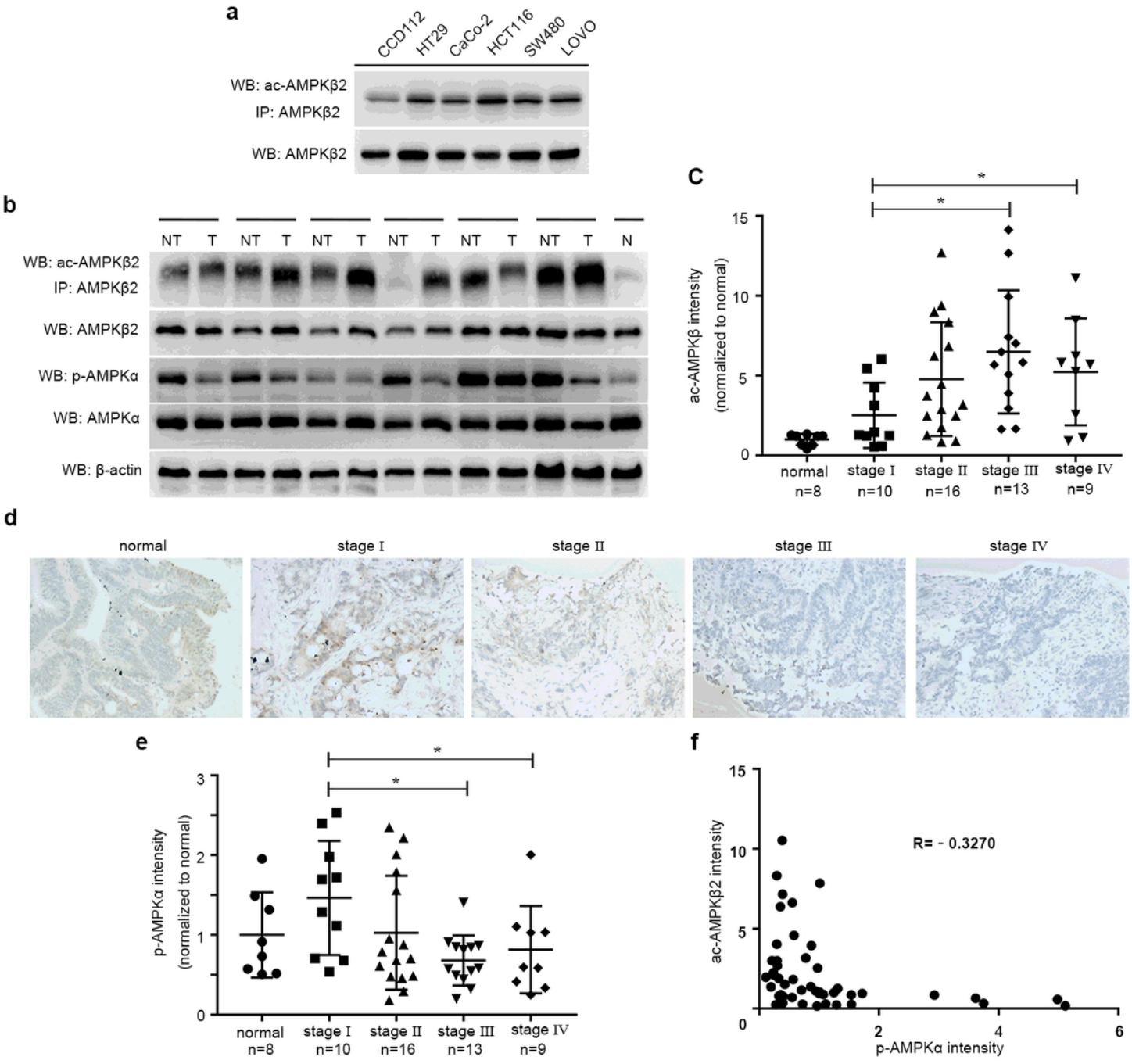

Figure 1

Evaluating phosphorylation and acetylation of AMPK in colon cancer patient specimens. a Expression of AMPKβ2 acetylation in CRC cell lines and the colon epithelial cell line CCD 112. b Immunoblot analysis of the acetylation levels in colorectal cancer patient samples (T) versus patient-matched normal colon tissues (NT) and normal colon tissues(N). Patient samples lysates were incubated with control IgG or a rabbit anti-AMPKβ2 antibody and immunoprecipitates were analyzed by Western Blot using anti-Acetylated-Lysine antibody. c Quantification of the acetylation levels of AMPKβ2 during human colorectal tumor progression. d IHC staining with an anti-p-AMPKα antibody was performed in normal colon and colon cancer specimens at different stages. Representative images are shown. Scale bar, 100 μm. e Quantification of the p-AMPKα levels during human colorectal tumor progression. f Correlation of expression of p-AMPKα and the acetylation level of AMPKβ2 was determined using Pearson's test (n=48). *P < 0.05, compared with control.

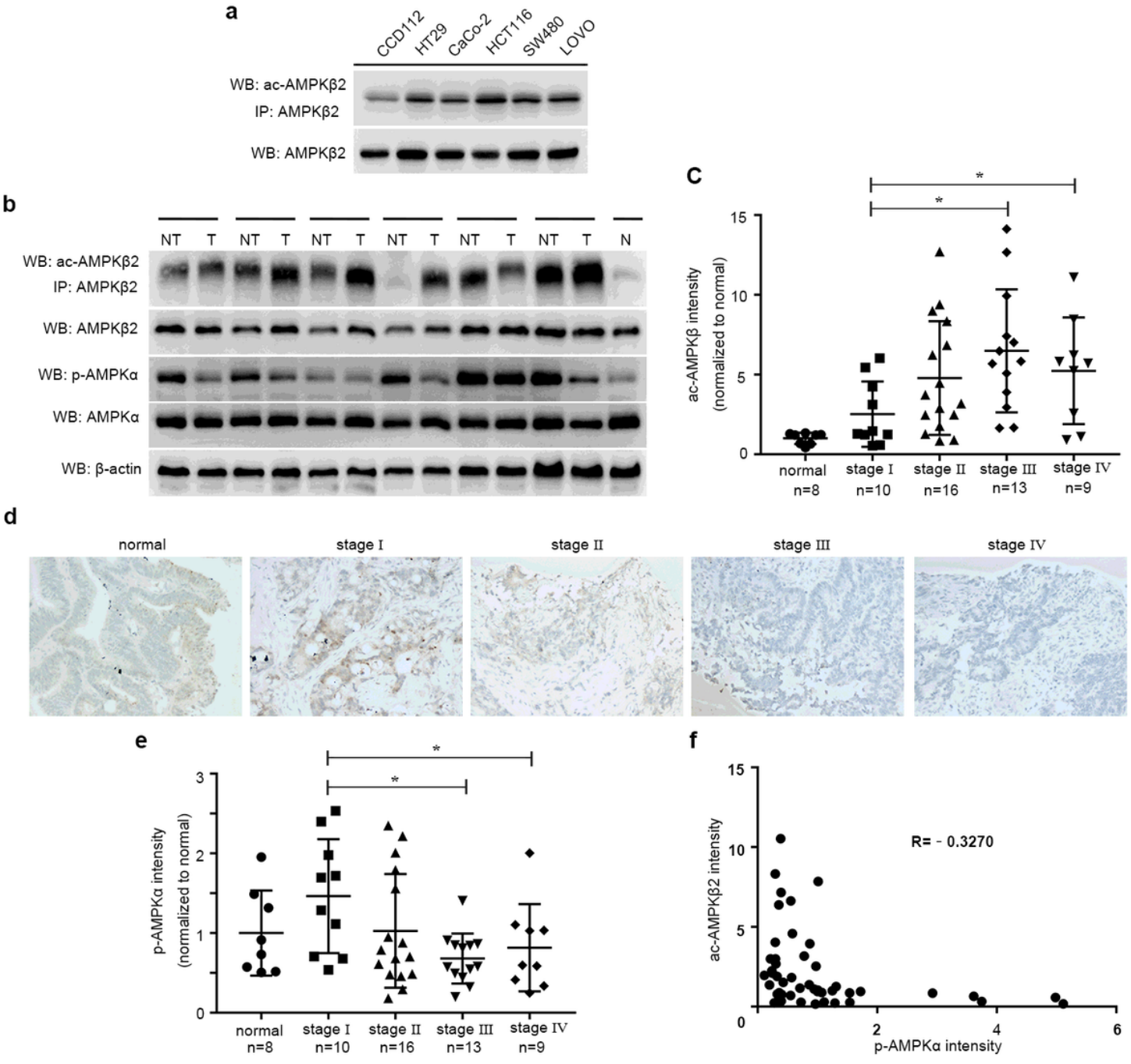

Figure 1

Evaluating phosphorylation and acetylation of AMPK in colon cancer patient specimens. a Expression of AMPKβ2 acetylation in CRC cell lines and the colon epithelial cell line CCD 112. b Immunoblot analysis of the acetylation levels in colorectal cancer patient samples (T) versus patient-matched normal colon tissues (NT) and normal colon tissues(N). Patient samples lysates were incubated with control IgG or a rabbit anti-AMPKβ2 antibody and immunoprecipitates were analyzed by Western Blot using anti-Acetylated-Lysine antibody. c Quantification of the acetylation levels of AMPKβ2 during human colorectal tumor progression. d IHC staining with an anti-p-AMPKα antibody was performed in normal colon and colon cancer specimens at different stages. Representative images are shown. Scale bar, 100 μm. e Quantification of the p-AMPKα levels during human colorectal tumor progression. f Correlation of expression of p-AMPKα and the acetylation level of AMPKβ2 was determined using Pearson's test (n=48). *P < 0.05, compared with control.

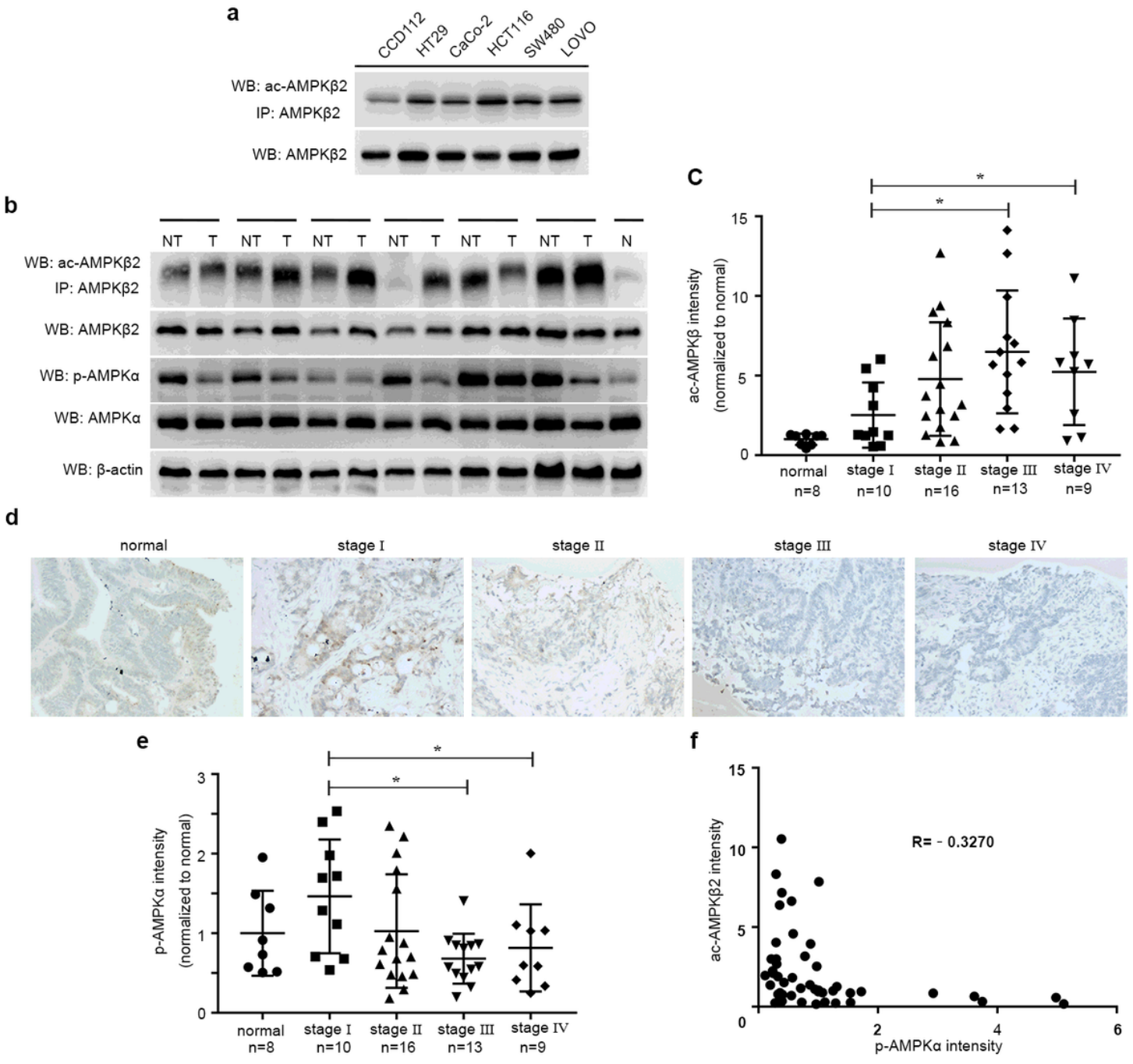

Figure 1

Evaluating phosphorylation and acetylation of AMPK in colon cancer patient specimens. a Expression of AMPKβ2 acetylation in CRC cell lines and the colon epithelial cell line CCD 112. b Immunoblot analysis of the acetylation levels in colorectal cancer patient samples (T) versus patient-matched normal colon tissues (NT) and normal colon tissues(N). Patient samples lysates were incubated with control IgG or a rabbit anti-AMPKβ2 antibody and immunoprecipitates were analyzed by Western Blot using anti-Acetylated-Lysine antibody. c Quantification of the acetylation levels of AMPKβ2 during human colorectal tumor progression. d IHC staining with an anti-p-AMPKα antibody was performed in normal colon and colon cancer specimens at different stages. Representative images are shown. Scale bar, 100 μm. e

Quantification of the p-AMPKα levels during human colorectal tumor progression. f Correlation of expression of p-AMPKα and the acetylation level of AMPKβ2 was determined using Pearson's test (n=48). *P < 0.05, compared with control.

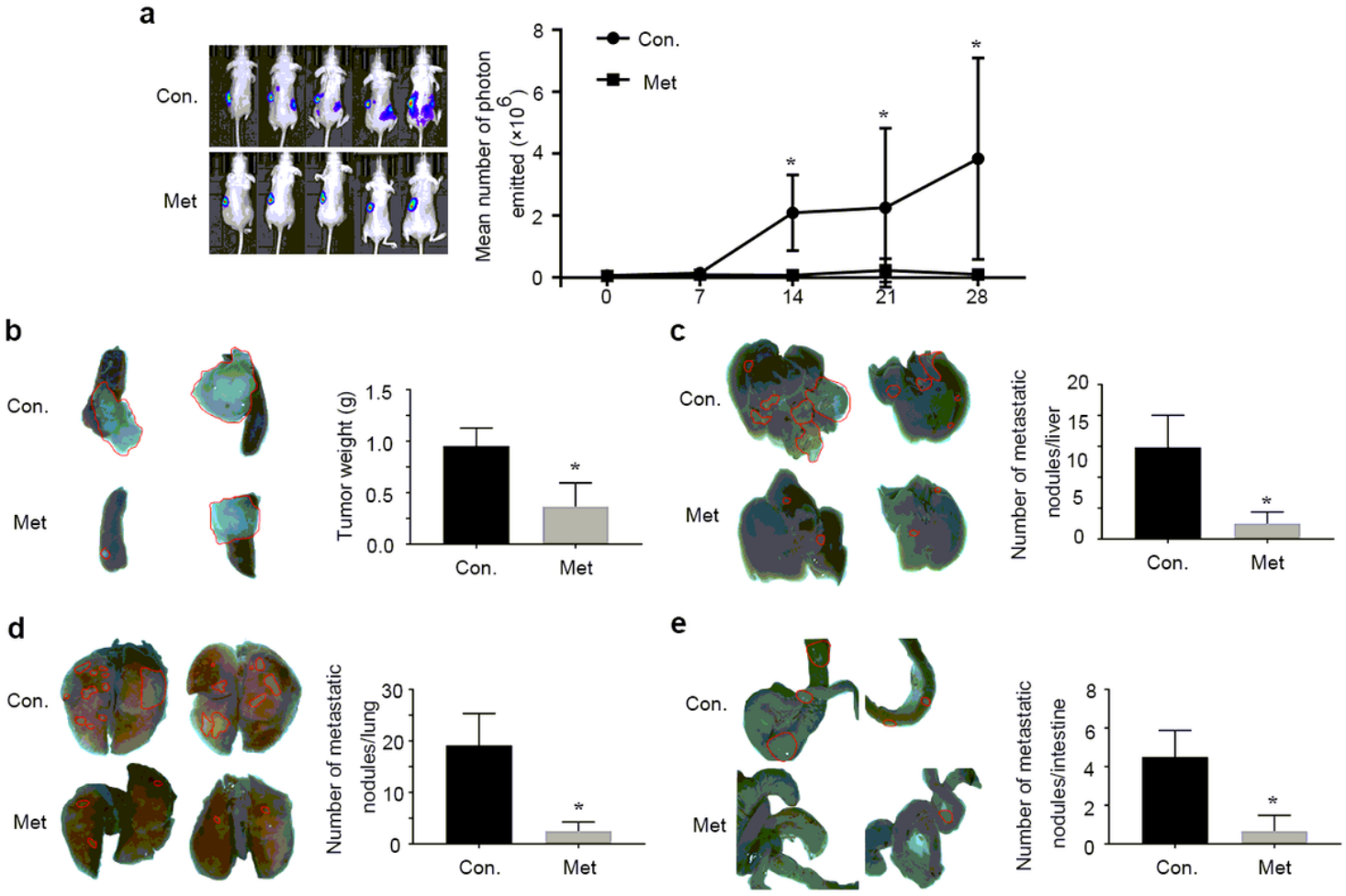

Figure 2

Significant antimetastatic effects of metformin in colorectal metastasis model. a Bioluminescence images from mice model (n = 6). Quantitative analysis of imaging signal intensity (photons/s/cm2/steradian) at the indicated time points. The signal intensities at the indicated time points were divided by the mean intensity from the time to treatment initiation. b Representative images of orthotopic tumors (indicated by the white arrow) with the spleen after treatment with the vehicle or metformin for 28 days. The average tumor weight in each group is shown. *P < 0.05, compared with the control group. c-e Representative images of liver, lung and colon. The metastatic nodules were counted. *P < 0.05, compared with the control group.

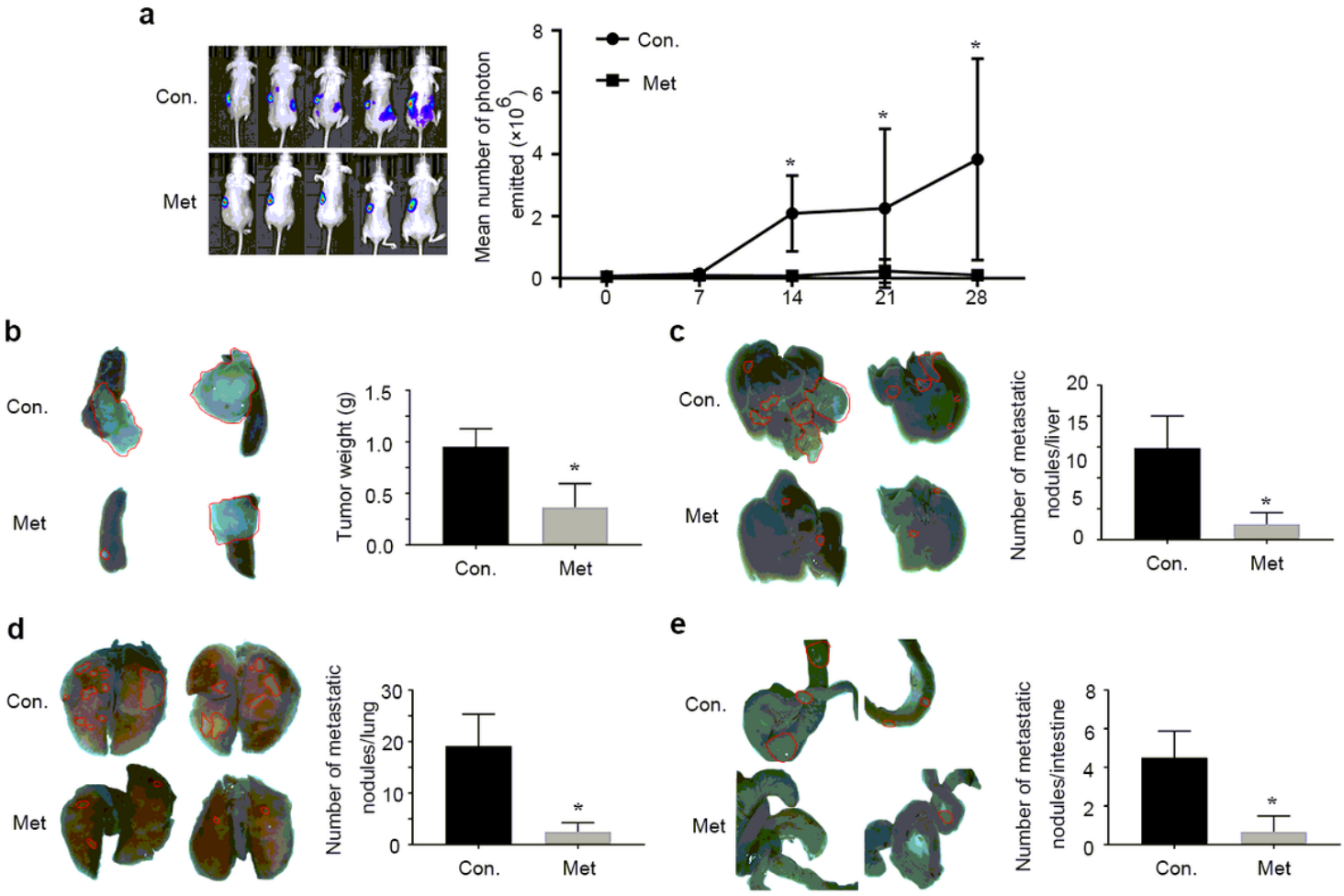

Figure 2

Significant antimetastatic effects of metformin in colorectal metastasis model. a Bioluminescence images from mice model (n = 6). Quantitative analysis of imaging signal intensity (photons/s/cm2/steradian) at the indicated time points. The signal intensities at the indicated time points were divided by the mean intensity from the time to treatment initiation. b Representative images of orthotopic tumors (indicated by the white arrow) with the spleen after treatment with the vehicle or metformin for 28 days. The average tumor weight in each group is shown. *P < 0.05, compared with the control group. c-e Representative images of liver, lung and colon. The metastatic nodules were counted. *P < 0.05, compared with the control group.

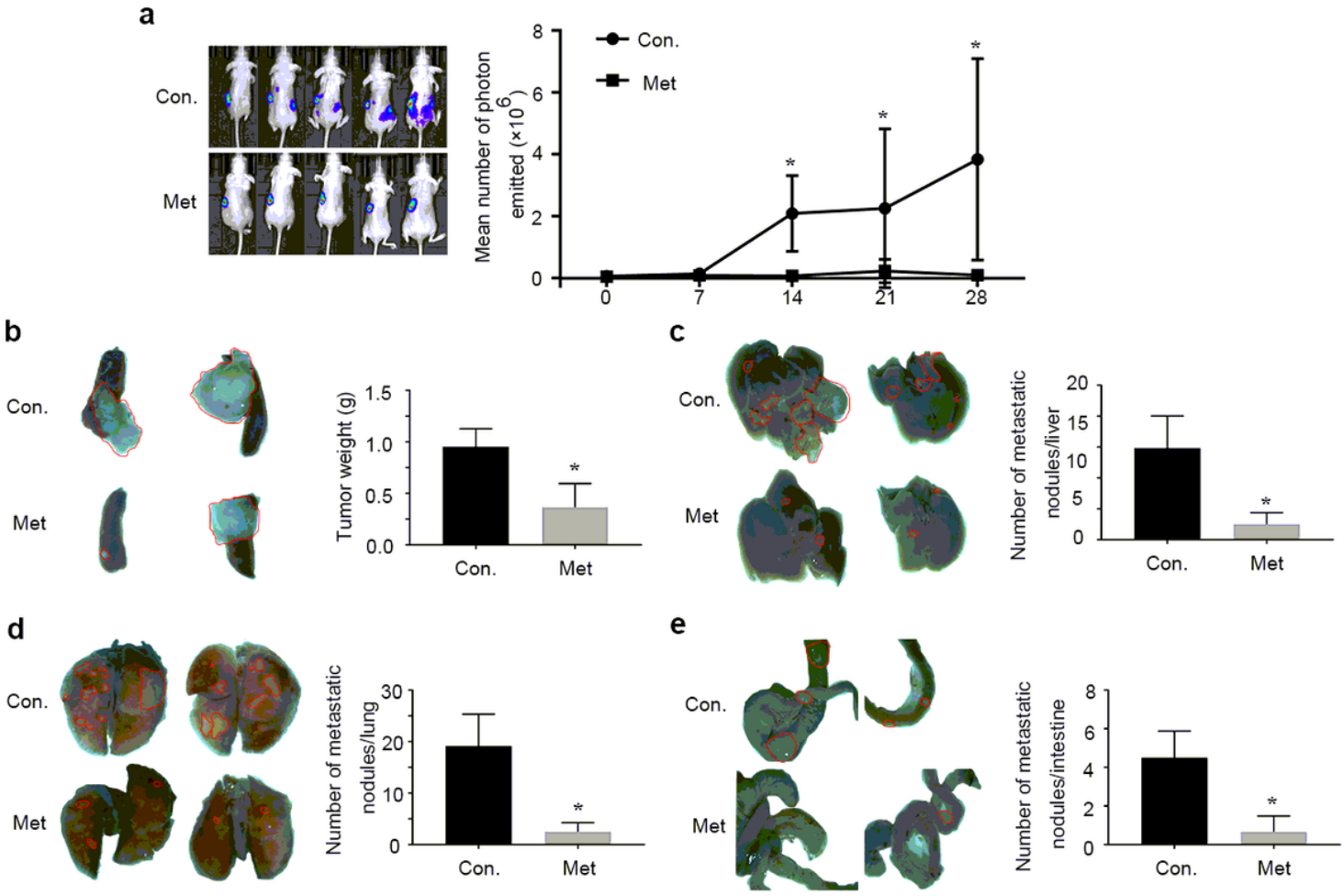

Figure 2

Significant antimetastatic effects of metformin in colorectal metastasis model. a Bioluminescence images from mice model (n = 6). Quantitative analysis of imaging signal intensity (photons/s/cm2/steradian) at the indicated time points. The signal intensities at the indicated time points were divided by the mean intensity from the time to treatment initiation. b Representative images of orthotopic tumors (indicated by the white arrow) with the spleen after treatment with the vehicle or metformin for 28 days. The average tumor weight in each group is shown. *P < 0.05, compared with the control group. c-e Representative images of liver, lung and colon. The metastatic nodules were counted. *P < 0.05, compared with the control group.

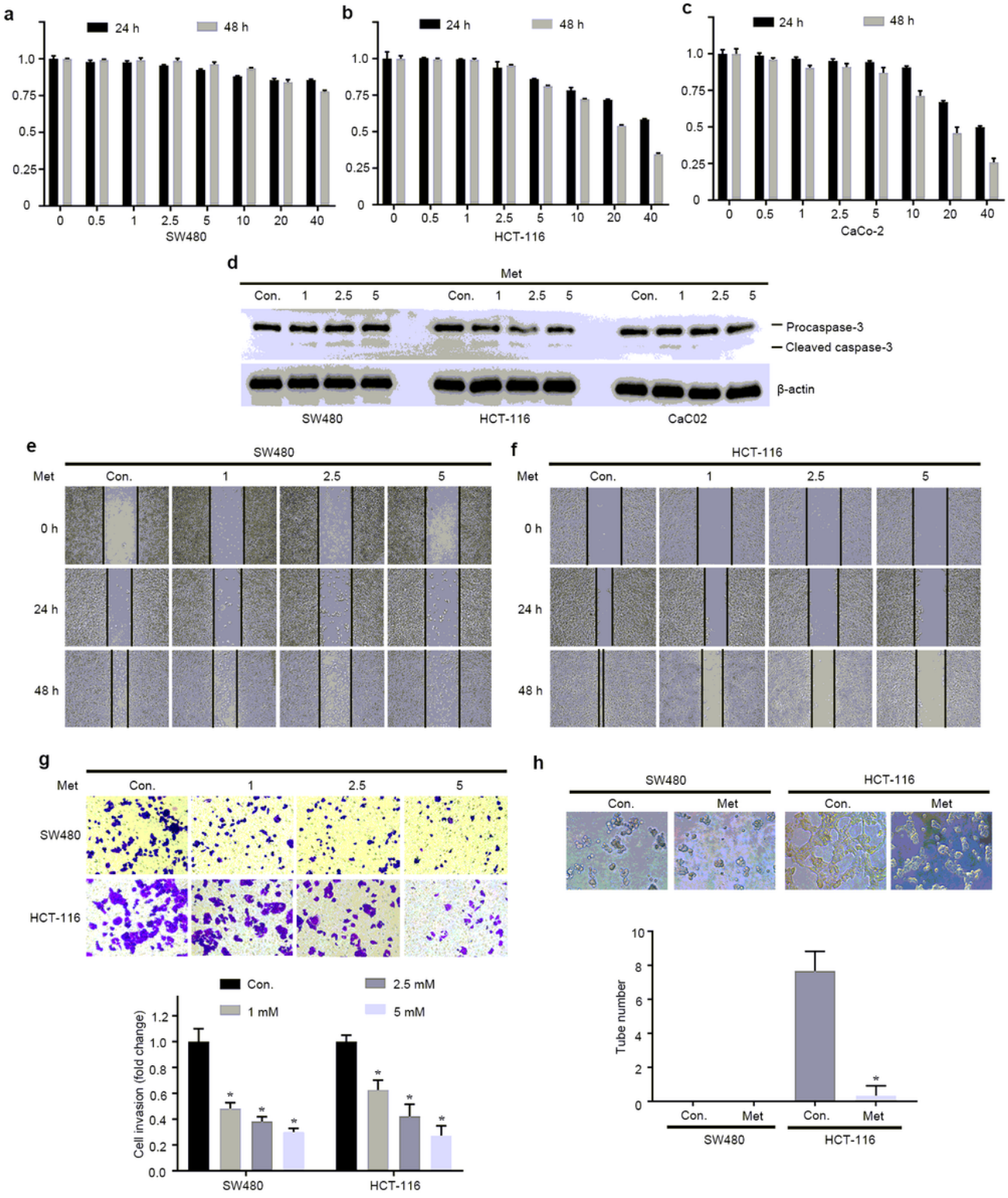

Figure 3

Metformin inhibits migration, invasion and the formation of vascular channels in CRC cells. a-c Effect of metformin on the proliferation of CRC cells. SW480, HCT-116 and CaCo-2 cells were treated with metformin (0-40 mM) for 24 and 48 hr. d SW480, HCT-116 and CaCo-2 cells were treated with metformin (0-5 mM) for 48 hr, and the level of Procaspase-3 and Cleaved caspase-3 were examined by Western blot. e and f Effect of metformin on wound closure in CRC cells. SW480 and HCT-116 cells were wounded and

were treated with metformin (0-5 mM) for 24 and 48 hr, and phase-contrast images of the wounds were taken. g the invasive capacities were determined by Transwell invasion assay. SW480 and HCT-116 cells were seeded into the upper chamber of the Transwell inserts. Representative invasive cells after 24 hr of incubation are shown. h SW480, HCT-116 cells cells were cultured on a three-dimensional matrix for 12 hr. the tube number was calculated. *P < 0.05, compared with the control group.

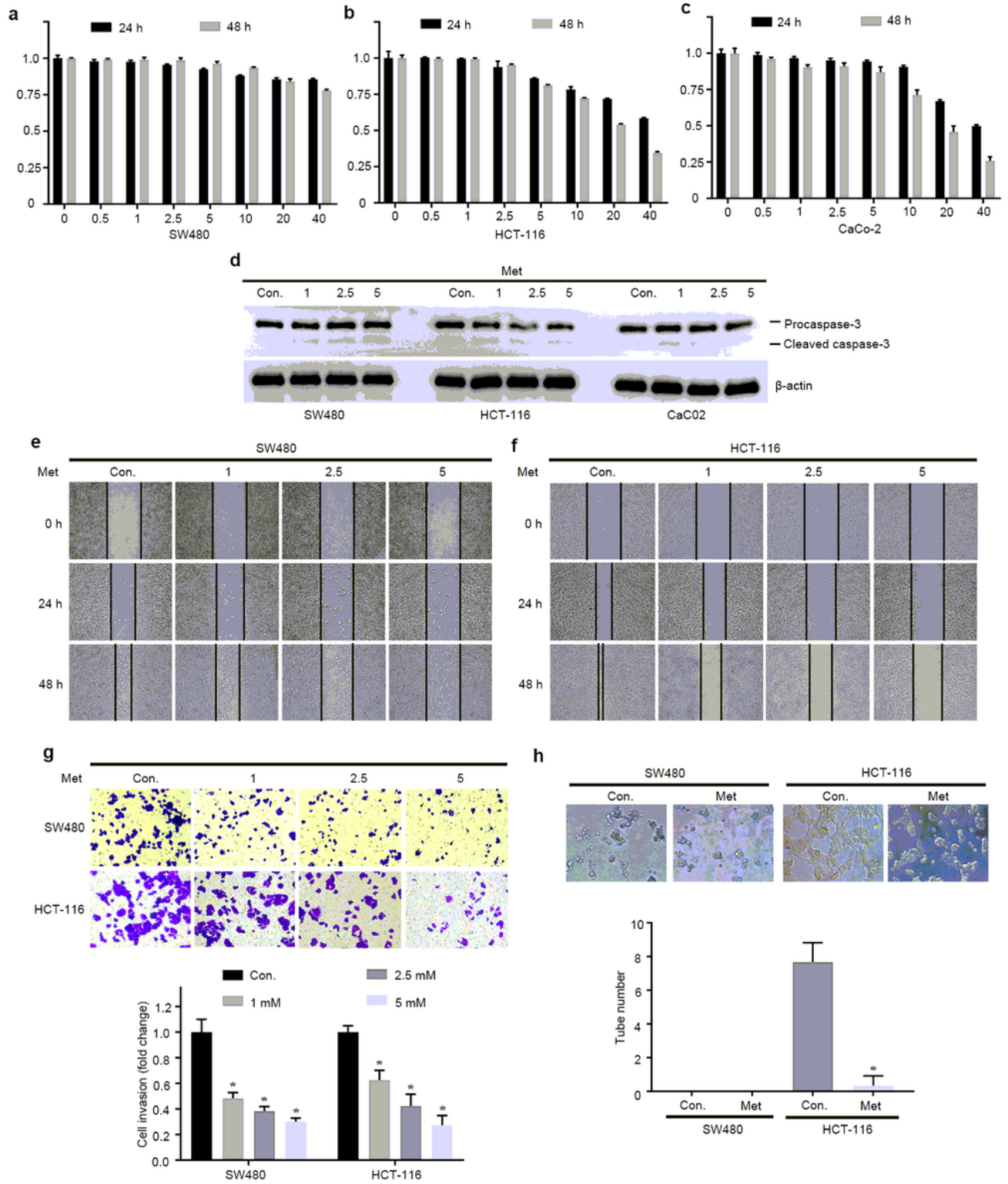

Figure 3

Metformin inhibits migration, invasion and the formation of vascular channels in CRC cells. a-c Effect of metformin on the proliferation of CRC cells. SW480, HCT-116 and CaCo-2 cells were treated with metformin (0-40 mM) for 24 and 48 hr. d SW480, HCT-116 and CaCo-2 cells were treated with metformin (0-5 mM) for 48 hr, and the level of Procaspase-3 and Cleaved caspase-3 were examined by Western blot. e and f Effect of metformin on wound closure in CRC cells. SW480 and HCT-116 cells were wounded and were treated with metformin (0-5 mM) for 24 and 48 hr, and phase-contrast images of the wounds were taken. g the invasive capacities were determined by Transwell invasion assay. SW480 and HCT-116 cells were seeded into the upper chamber of the Transwell inserts. Representative invasive cells after 24 hr of incubation are shown. h SW480, HCT-116 cells cells were cultured on a three-dimensional matrix for 12 hr. the tube number was calculated. *P < 0.05, compared with the control group.

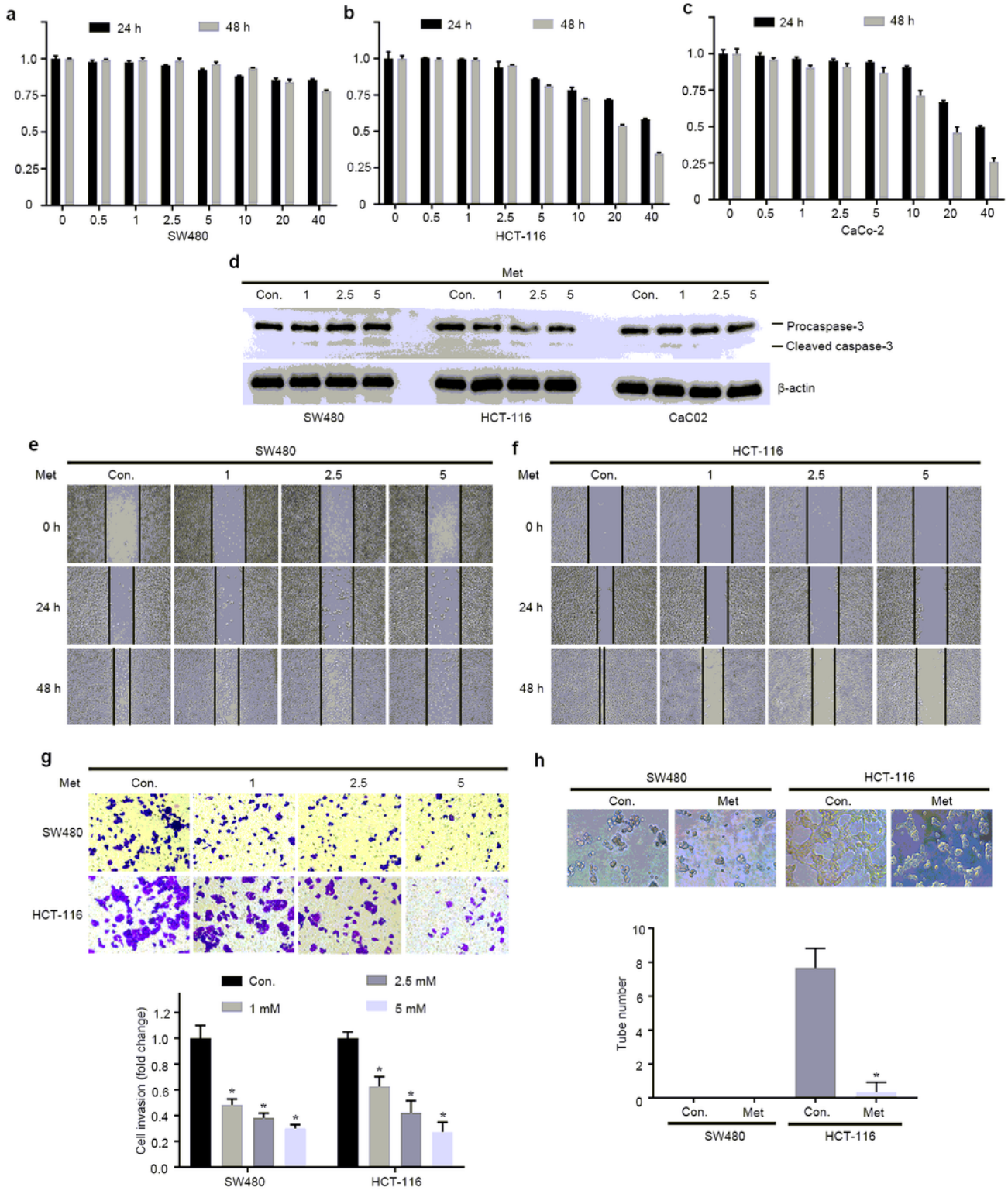

Figure 3

Metformin inhibits migration, invasion and the formation of vascular channels in CRC cells. a-c Effect of metformin on the proliferation of CRC cells. SW480, HCT-116 and CaCo-2 cells were treated with metformin (0-40 mM) for 24 and 48 hr. d SW480, HCT-116 and CaCo-2 cells were treated with metformin (0-5 mM) for 48 hr, and the level of Procaspase-3 and Cleaved caspase-3 were examined by Western blot. e and f Effect of metformin on wound closure in CRC cells. SW480 and HCT-116 cells were wounded and

were treated with metformin (0-5 mM) for 24 and 48 hr, and phase-contrast images of the wounds were taken. g the invasive capacities were determined by Transwell invasion assay. SW480 and HCT-116 cells were seeded into the upper chamber of the Transwell inserts. Representative invasive cells after 24 hr of incubation are shown. h SW480, HCT-116 cells cells were cultured on a three-dimensional matrix for 12 hr. the tube number was calculated. *P < 0.05, compared with the control group.

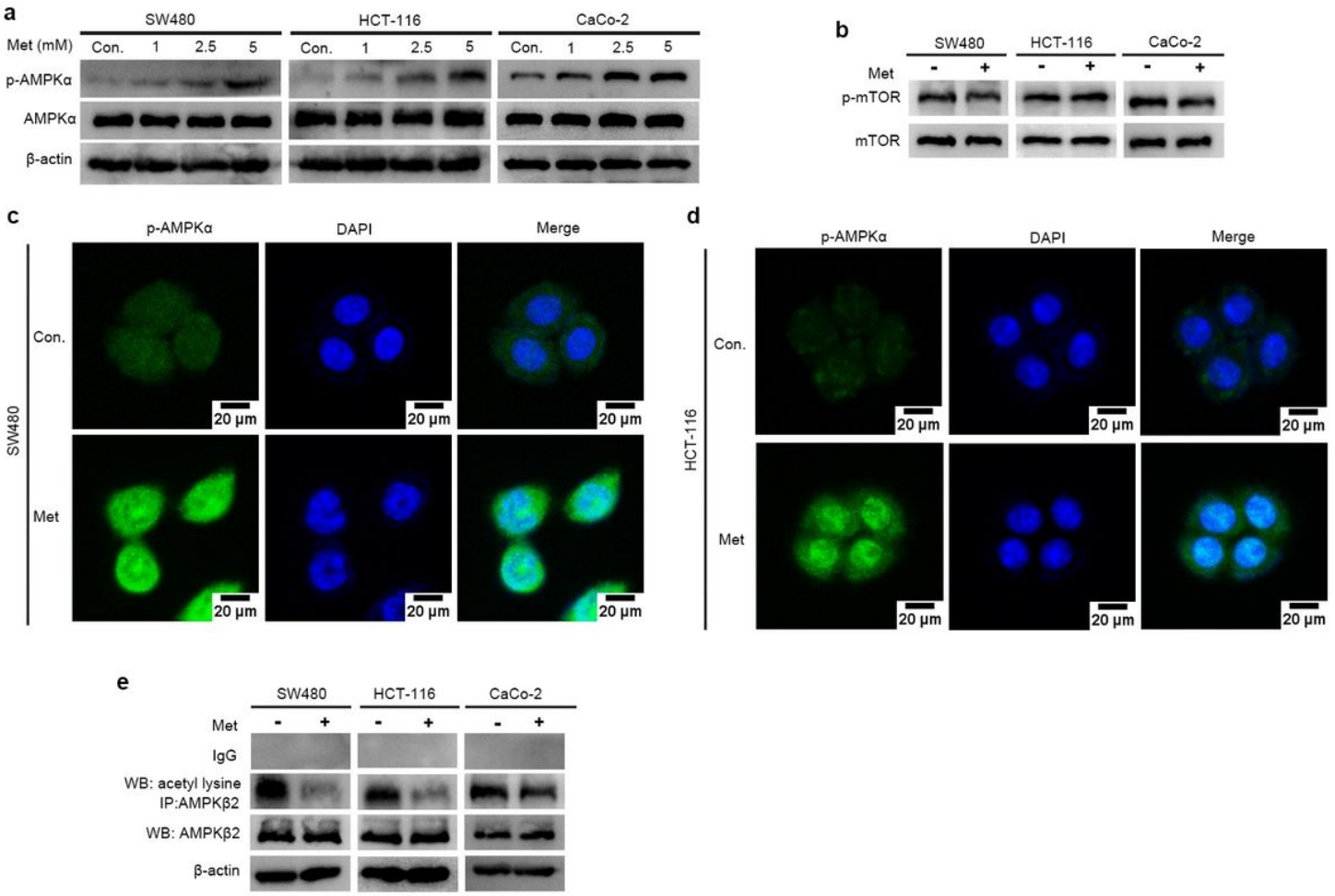

Figure 4

Metformin activates AMPK and reduce acetylation level of AMPK. a SW480, HCT-116 and CaCo-2 cells were treated with metformin (0-5 mM) for 24 hr, and the level of p-AMPK was examined by Western blot. b SW480, HCT-116 and CaCo-2 cells were treated with vehicle or metformin (5 mM) for 24 hr, the level of p-mTOR and mTOR was examined by Western blot. c and d The subcellular location of p-AMPKα in SW480 and HCT-116 cells were detected by immunofluorescence staining using the p-AMPKα antibody, and photographed by a fluorescence microscope. e SW480, HCT-116 and CaCo-2 cells were treated with vehicle or metformin (5 mM) for 24 hr. Lysates were incubated with control IgG or a rabbit anti-AMPKβ2 antibody and immunoprecipitates were analyzed by Western Blot using anti-Acetylated-Lysine antibody.

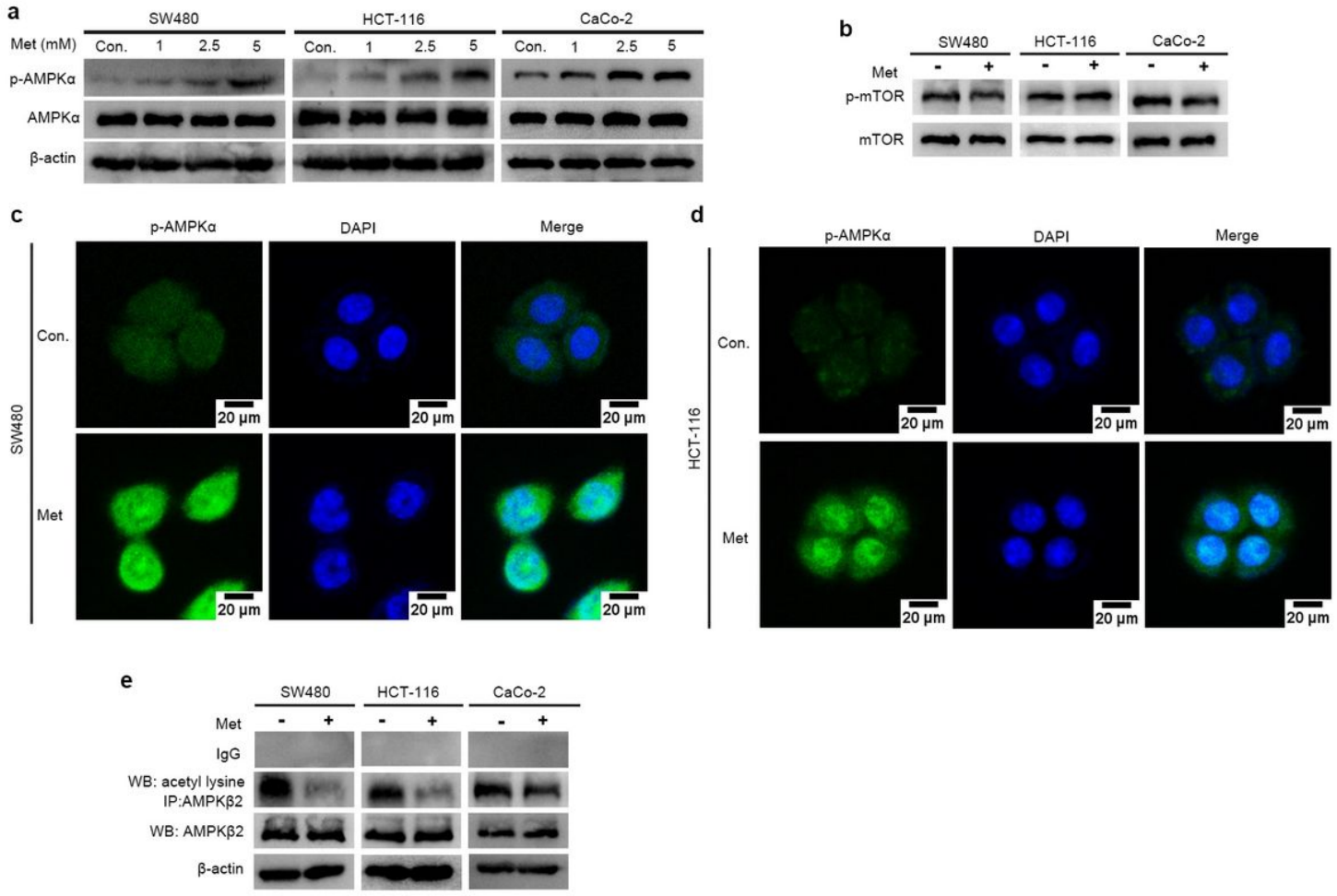

Figure 4

Metformin activates AMPK and reduce acetylation level of AMPK. a SW480, HCT-116 and CaCo-2 cells were treated with metformin (0-5 mM) for 24 hr, and the level of p-AMPK was examined by Western blot. b SW480, HCT-116 and CaCo-2 cells were treated with vehicle or metformin (5 mM) for 24 hr, the level of p-mTOR and mTOR was examined by Western blot. c and d The subcellular location of p-AMPKα in SW480 and HCT-116 cells were detected by immunofluorescence staining using the p-AMPKα antibody, and photographed by a fluorescence microscope. e SW480, HCT-116 and CaCo-2 cells were treated with vehicle or metformin (5 mM) for 24 hr. Lysates were incubated with control IgG or a rabbit anti-AMPKβ2 antibody and immunoprecipitates were analyzed by Western Blot using anti-Acetylated-Lysine antibody.

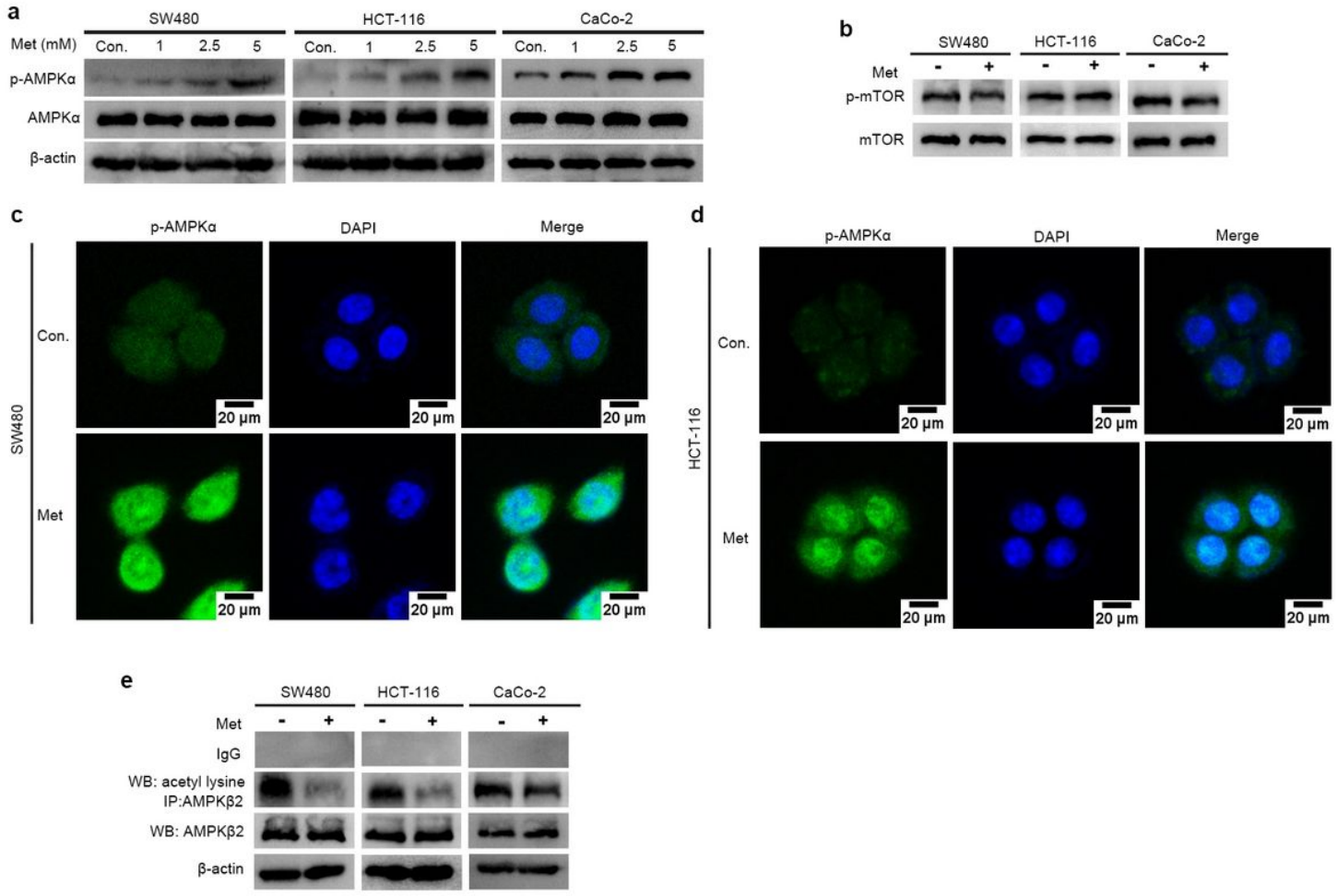

Figure 4

Metformin activates AMPK and reduce acetylation level of AMPK. a SW480, HCT-116 and CaCo-2 cells were treated with metformin (0-5 mM) for 24 hr, and the level of p-AMPK was examined by Western blot. b SW480, HCT-116 and CaCo-2 cells were treated with vehicle or metformin (5 mM) for 24 hr, the level of p-mTOR and mTOR was examined by Western blot. c and d The subcellular location of p-AMPKα in SW480 and HCT-116 cells were detected by immunofluorescence staining using the p-AMPKα antibody, and photographed by a fluorescence microscope. e SW480, HCT-116 and CaCo-2 cells were treated with vehicle or metformin (5 mM) for 24 hr. Lysates were incubated with control IgG or a rabbit anti-AMPKβ2 antibody and immunoprecipitates were analyzed by Western Blot using anti-Acetylated-Lysine antibody.

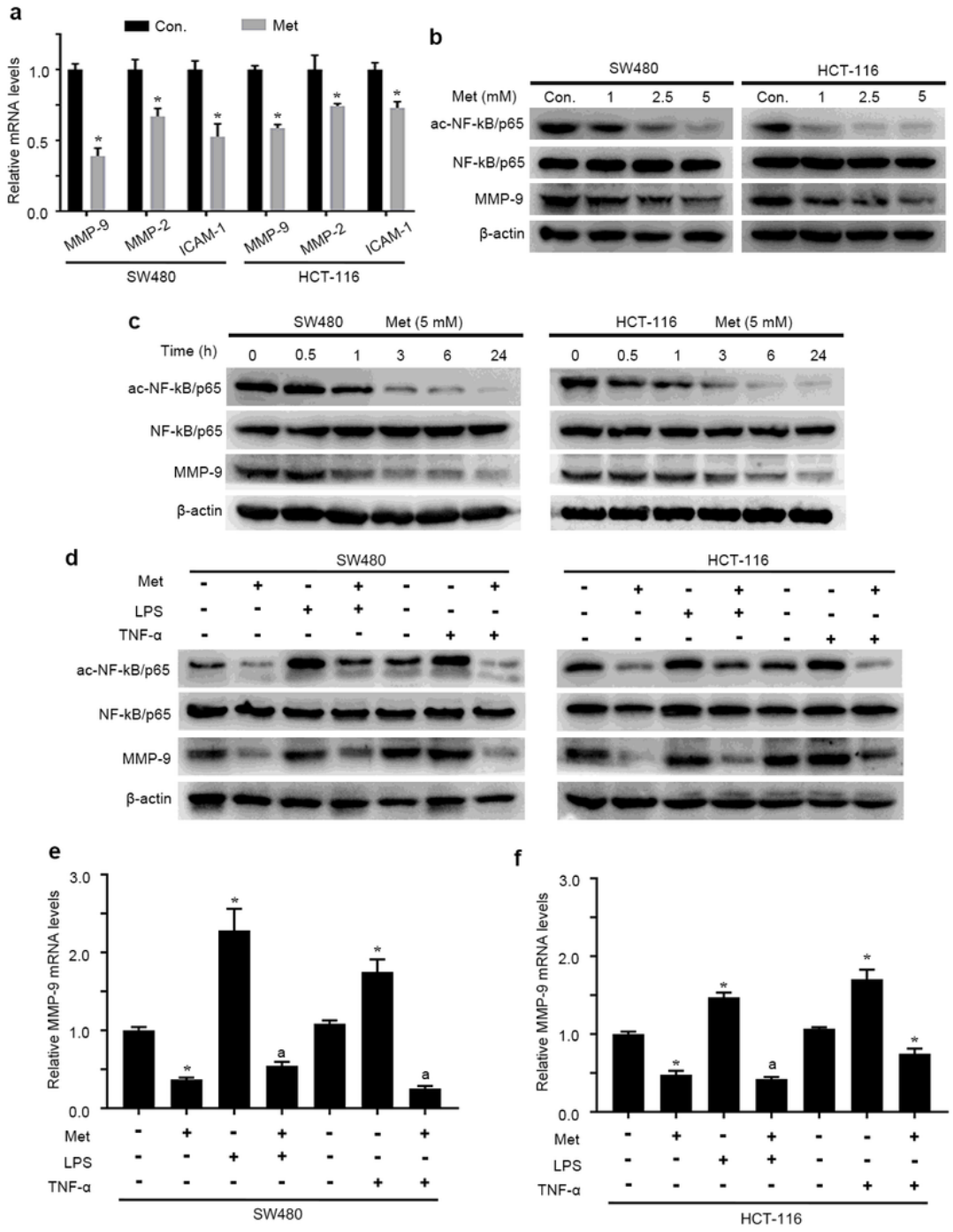

Figure 5

Metformin inhibits the transcriptional activity of NF-kB/p65. a SW480 and HCT-116 cells were treated with the vehicle or metformin (5 mM) for 24 hr, and reverse transcription polymerase chain reaction (PCR) was to detect the MMP-9 MMP-2 and ICAM-1 mRNA expressions. Quantitative results of MMP-9 MMP-2 and ICAM-1 mRNA were adjust to GADPH mRNA levels. *P < 0.05, compared with the control group. b and c SW480 and HCT-116 cells were treated with the vehicle or metformin for the indicated time and

concentration, and a Western blot was performed using indicated antibody d, e and f SW480 and HCT-116 cells were treated with the vehicle or metformin (5 mM) for 1 hr, before indicated time, cells were treated with 1 μg/mL LPS or 2.5 ng/mL TNF-α for 0.5 hr, then Western blot and PCR were performed. *P < 0.05, compared with the control group; aP < 0.05, compared with the LPS group; #P < 0.05, compared with the control group.

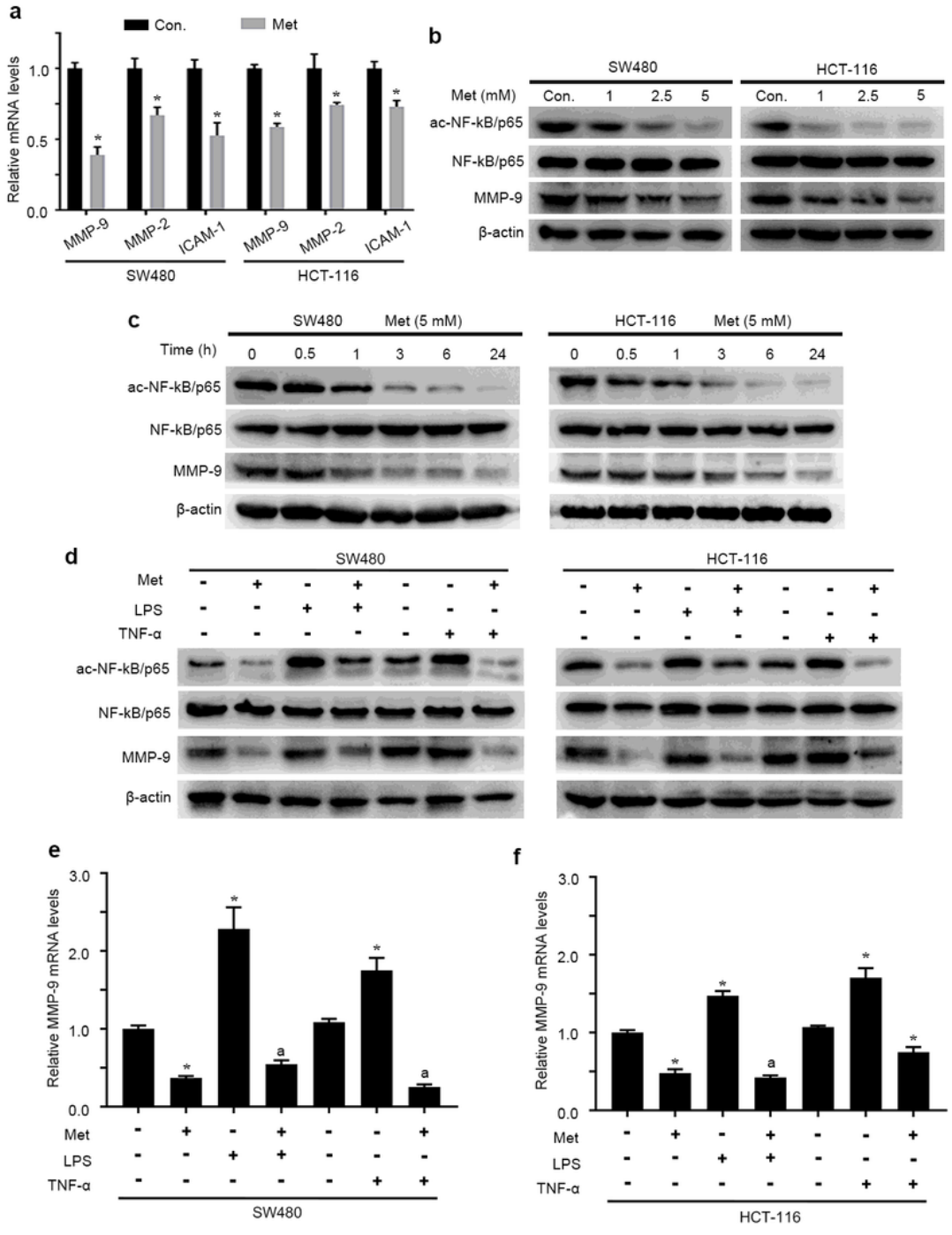

Figure 5

Metformin inhibits the transcriptional activity of NF-kB/p65. a SW480 and HCT-116 cells were treated with the vehicle or metformin (5 mM) for 24 hr, and reverse transcription polymerase chain reaction (PCR) was to detect the MMP-9 MMP-2 and ICAM-1 mRNA expressions. Quantitative results of MMP-9 MMP-2 and ICAM-1 mRNA were adjust to GADPH mRNA levels. *P < 0.05, compared with the control group. b and c SW480 and HCT-116 cells were treated with the vehicle or metformin for the indicated time and concentration, and a Western blot was performed using indicated antibody d, e and f SW480 and HCT-116 cells were treated with the vehicle or metformin (5 mM) for 1 hr, before indicated time, cells were treated with 1 μg/mL LPS or 2.5 ng/mL TNF-α for 0.5 hr, then Western blot and PCR were performed. *P < 0.05, compared with the control group; aP < 0.05, compared with the LPS group; #P < 0.05, compared with the control group.

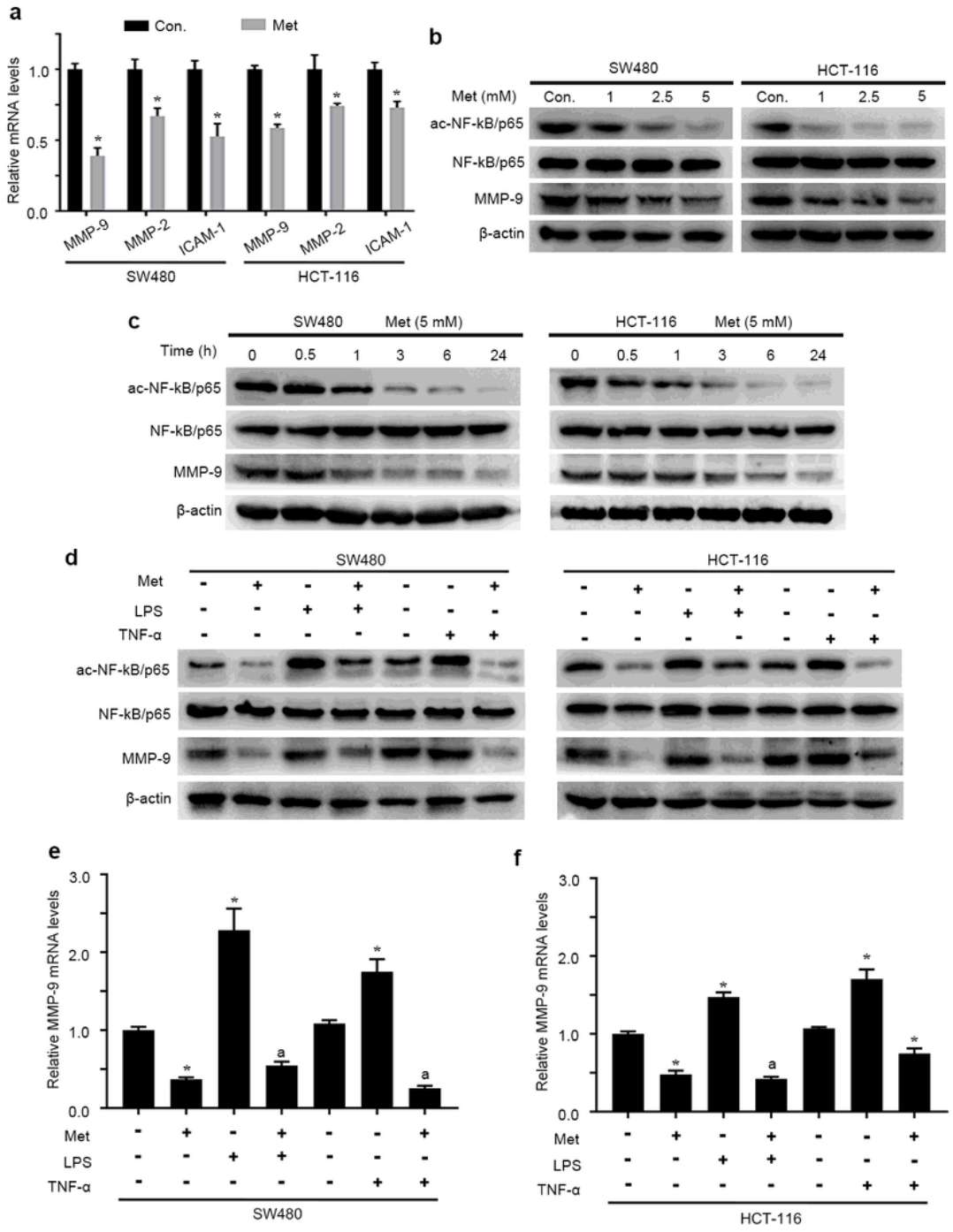

Figure 5

Metformin inhibits the transcriptional activity of NF-kB/p65. a SW480 and HCT-116 cells were treated with the vehicle or metformin (5 mM) for 24 hr, and reverse transcription polymerase chain reaction (PCR) was to detect the MMP-9 MMP-2 and ICAM-1 mRNA expressions. Quantitative results of MMP-9 MMP-2 and ICAM-1 mRNA were adjust to GADPH mRNA levels. *P < 0.05, compared with the control group. b and c SW480 and HCT-116 cells were treated with the vehicle or metformin for the indicated time and

concentration, and a Western blot was performed using indicated antibody d, e and f SW480 and HCT-116 cells were treated with the vehicle or metformin (5 mM) for 1 hr, before indicated time, cells were treated with 1 μg/mL LPS or 2.5 ng/mL TNF-α for 0.5 hr, then Western blot and PCR were performed. *P < 0.05, compared with the control group; aP < 0.05, compared with the LPS group; #P < 0.05, compared with the control group.

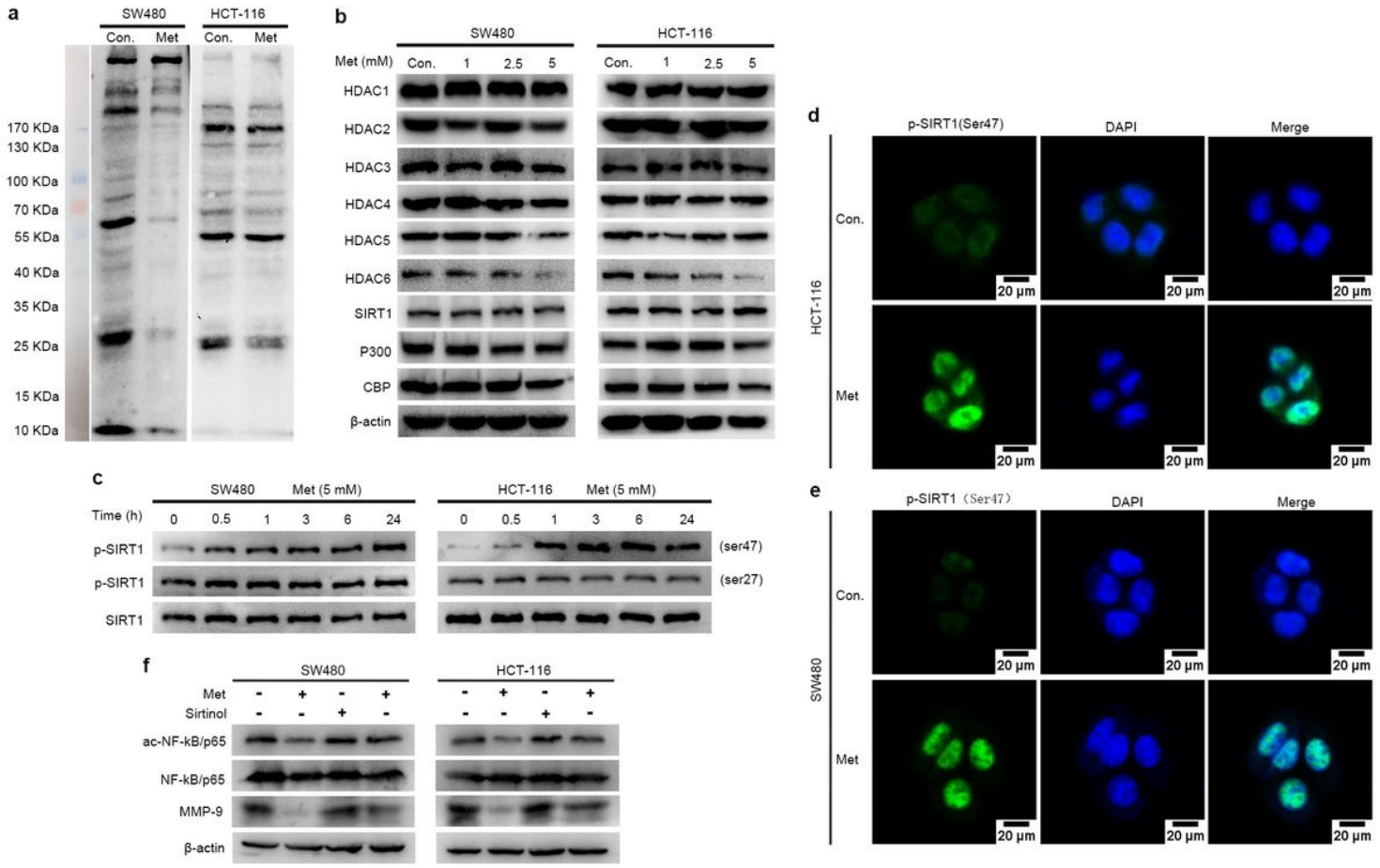

Figure 6

Metformin enhances phosphorylation of SIRT1 (Ser47) to deacetylate NF-kB/p65. a SW480 and HCT-116 cells were treated with vehicle or metformin (5 mM) for 24 hr, whole cell lysates were analyzed by Western Blot using anti-Acetylated-Lysine antibody. b SW480 and HCT-116 cells were treated with metformin (0-5 mM) for 24 hr, and HDAC1, HDAC2, HDAC3, HDAC4, HDAC5, HDAC6, SIRT1, p300 and CBP levels were detected by Western Blot. c SW480 and HCT-116 cells were treated with the vehicle or metformin for the indicated time, and a Western blot was performed to detect the phosphorylation of SIRT1(Ser27 and Ser47). d and e The subcellular location of p-SIRT1(Ser47) in SW480 and HCT-116 cells were detected by immunofluorescence staining using the p-SIRT1 antibody, and photographed by a fluorescence microscope. f SW480 and HCT-116 cells were treated with the vehicle or metformin (5 mM) for 24 hr, before indicated time, cells were pretreated with 20μM Sirtinol for 1 hr, then a Western blot was performed using the indicated antibodies.

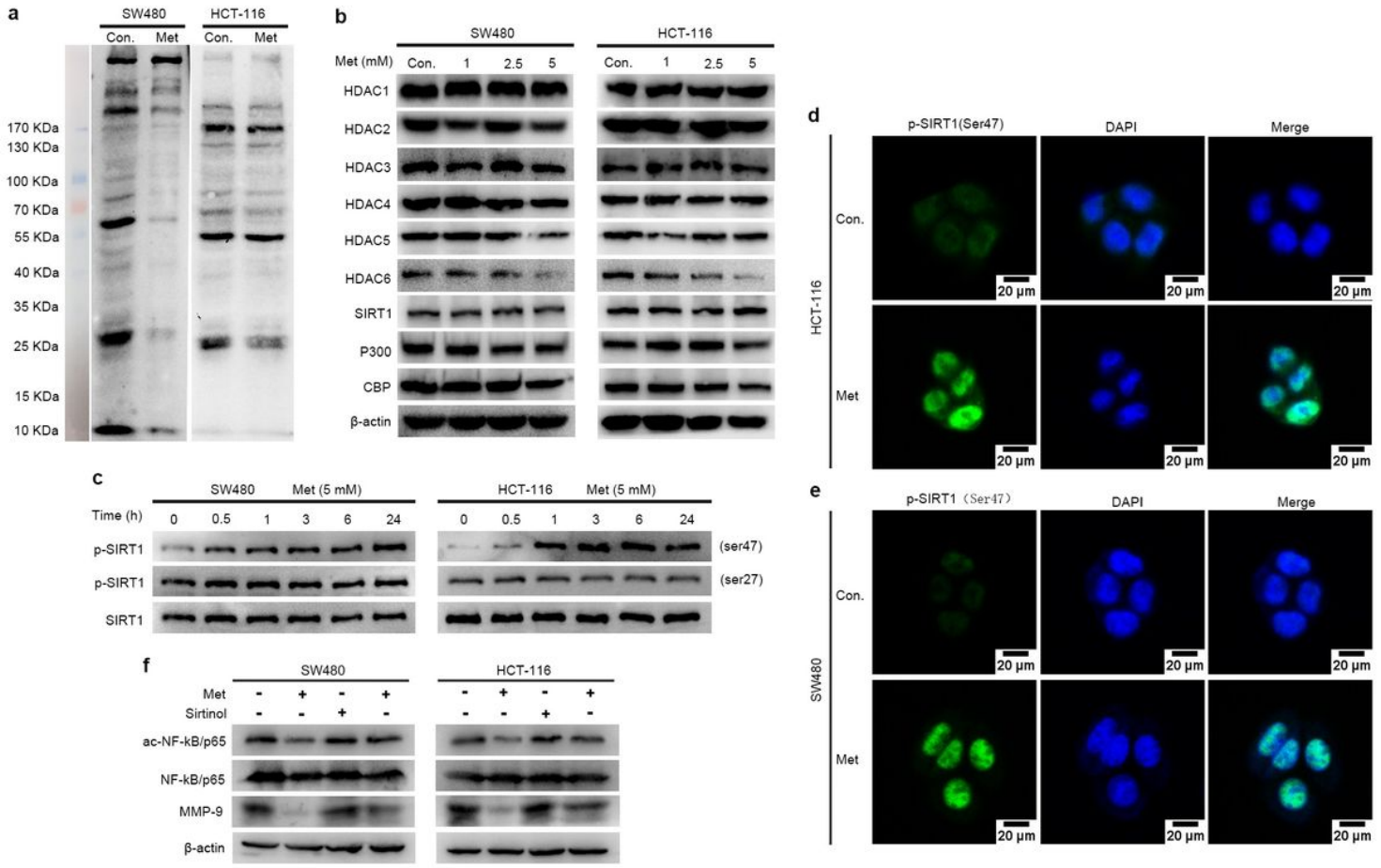

Figure 6

Metformin enhances phosphorylation of SIRT1 (Ser47) to deacetylate NF-kB/p65. a SW480 and HCT-116 cells were treated with vehicle or metformin (5 mM) for 24 hr, whole cell lysates were analyzed by Western Blot using anti-Acetylated-Lysine antibody. b SW480 and HCT-116 cells were treated with metformin (0-5 mM) for 24 hr, and HDAC1, HDAC2, HDAC3, HDAC4, HDAC5, HDAC6, SIRT1, p300 and CBP levels were detected by Western Blot. c SW480 and HCT-116 cells were treated with the vehicle or metformin for the indicated time, and a Western blot was performed to detect the phosphorylation of SIRT1(Ser27 and Ser47). d and e The subcellular location of p-SIRT1(Ser47) in SW480 and HCT-116 cells were detected by immunofluorescence staining using the p-SIRT1 antibody, and photographed by a fluorescence microscope. f SW480 and HCT-116 cells were treated with the vehicle or metformin (5 mM) for 24 hr, before indicated time, cells were pretreated with 20μM Sirtinol for 1 hr, then a Western blot was performed using the indicated antibodies.

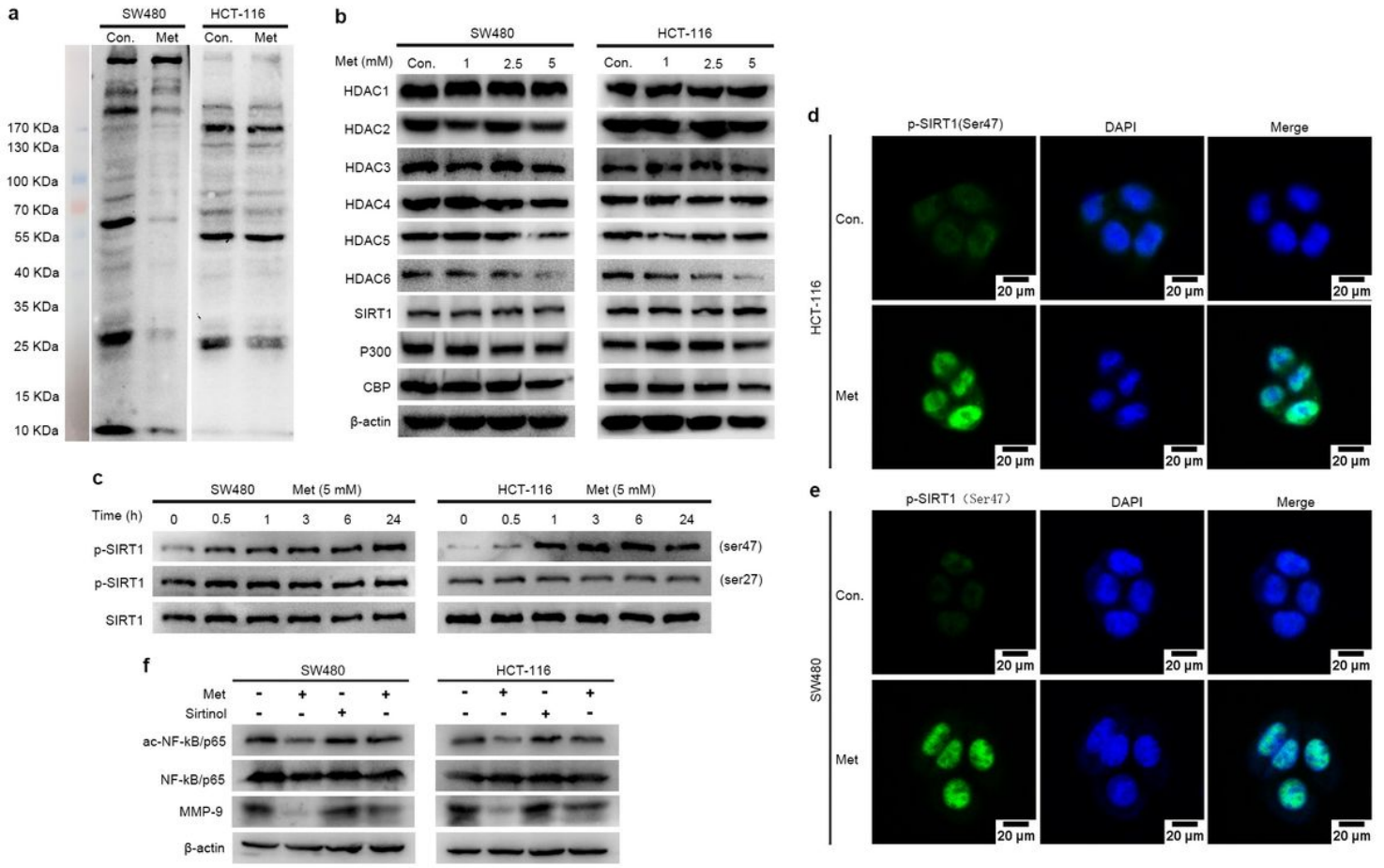

Figure 6

Metformin enhances phosphorylation of SIRT1 (Ser47) to deacetylate NF-kB/p65. a SW480 and HCT-116 cells were treated with vehicle or metformin (5 mM) for 24 hr, whole cell lysates were analyzed by Western Blot using anti-Acetylated-Lysine antibody. b SW480 and HCT-116 cells were treated with metformin (0-5 mM) for 24 hr, and HDAC1, HDAC2, HDAC3, HDAC4, HDAC5, HDAC6, SIRT1, p300 and CBP levels were detected by Western Blot. c SW480 and HCT-116 cells were treated with the vehicle or metformin for the indicated time, and a Western blot was performed to detect the phosphorylation of SIRT1(Ser27 and Ser47). d and e The subcellular location of p-SIRT1(Ser47) in SW480 and HCT-116 cells were detected by immunofluorescence staining using the p-SIRT1 antibody, and photographed by a fluorescence microscope. f SW480 and HCT-116 cells were treated with the vehicle or metformin (5 mM) for 24 hr, before indicated time, cells were pretreated with 20μM Sirtinol for 1 hr, then a Western blot was performed using the indicated antibodies.

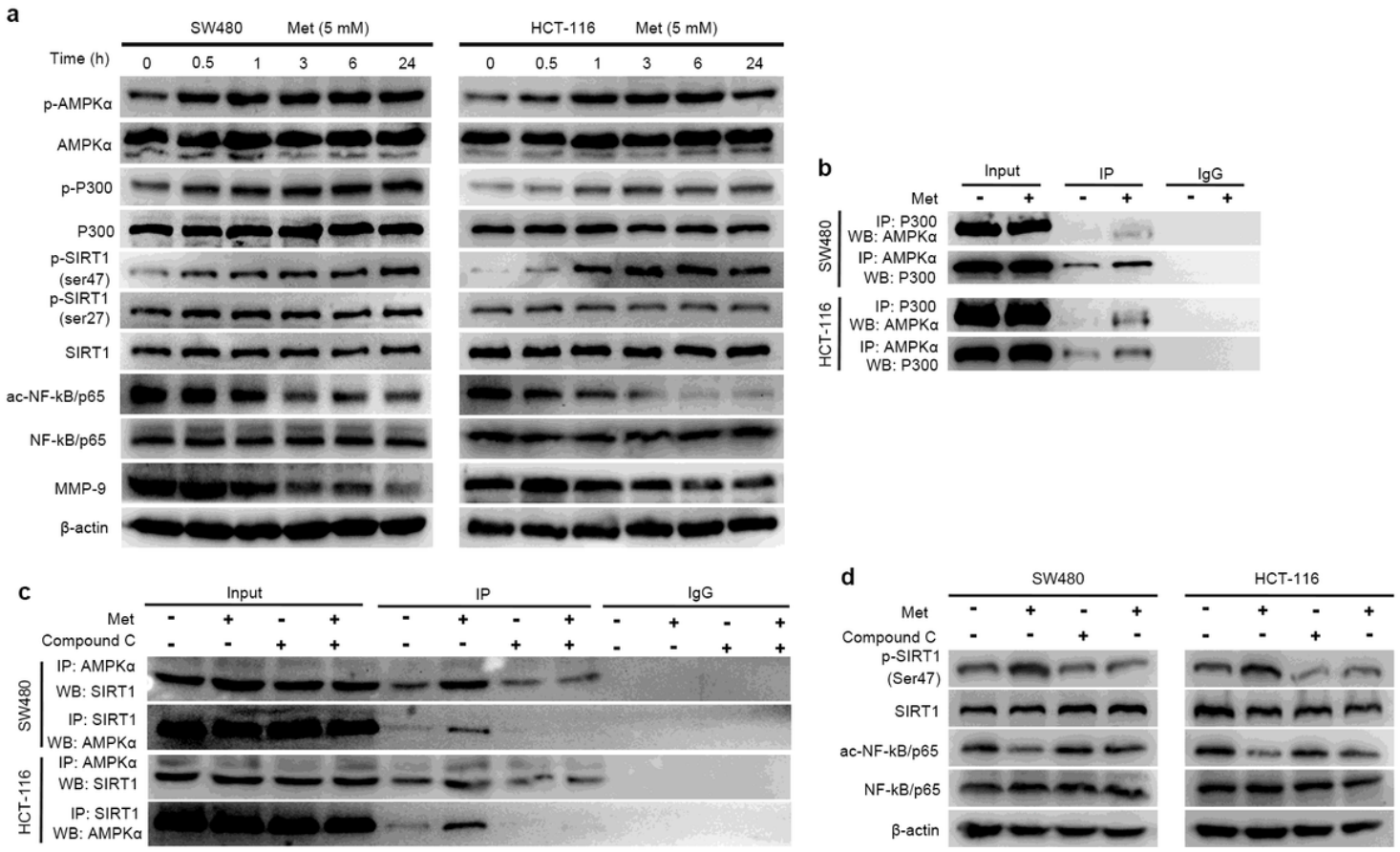

Figure 7

Metformin activates SIRT1 by inducing AMPK phosphorylation. a SW480 and HCT-116 cells were treated with the vehicle or metformin for the indicated time, and a Western blot was performed using indicated antibody. b SW480 and HCT-116 cells were treated with the vehicle or metformin (5 mM) for 24 hr. Lysates were incubated with control IgG, a rabbit anti-AMPKα antibody or a mouse anti-P300 antibody, and immunoprecipitates were analyzed by Western Blot. cSW480 and HCT-116 cells were treated with the vehicle or metformin (5 mM) in the presence or absence of Compound C (10 μM), then cells were lysed and immunoprecipitated using SIRT1 and AMPKα antibodies. The protein level was detected by Western blot using indicted antibodies. d SW480 and HCT-116 cells were treated with the vehicle or metformin (5 mM) in the presence or absence of Compound C (10 μM), and a Western blot was performed using indicated antibody.

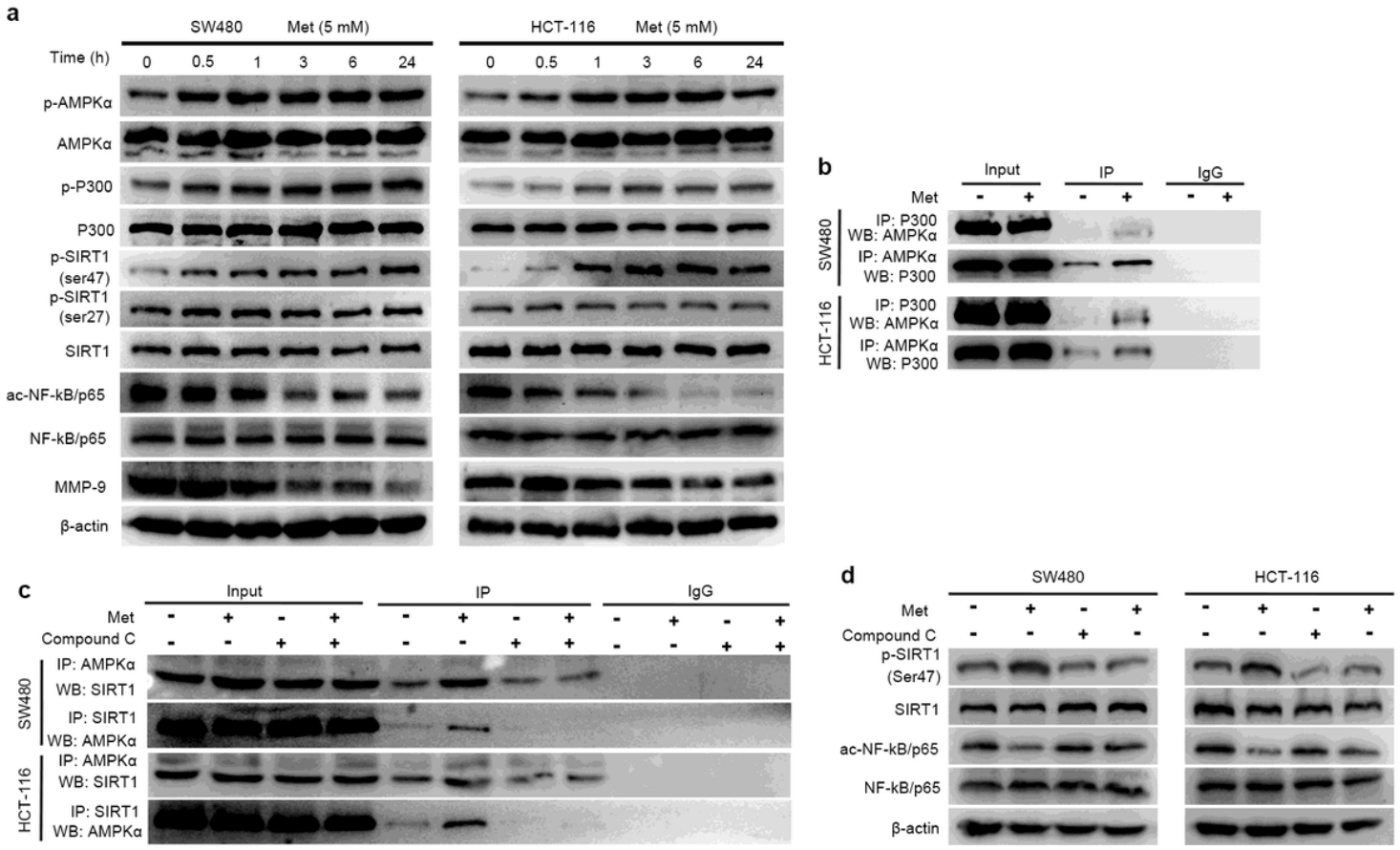

Figure 7

Metformin activates SIRT1 by inducing AMPK phosphorylation. a SW480 and HCT-116 cells were treated with the vehicle or metformin for the indicated time, and a Western blot was performed using indicated antibody. b SW480 and HCT-116 cells were treated with the vehicle or metformin (5 mM) for 24 hr. Lysates were incubated with control IgG, a rabbit anti-AMPKα antibody or a mouse anti-P300 antibody, and immunoprecipitates were analyzed by Western Blot. cSW480 and HCT-116 cells were treated with the vehicle or metformin (5 mM) in the presence or absence of Compound C (10 μM), then cells were lysed and immunoprecipitated using SIRT1 and AMPKα antibodies. The protein level was detected by Western blot using indicted antibodies. d SW480 and HCT-116 cells were treated with the vehicle or metformin (5 mM) in the presence or absence of Compound C (10 μM), and a Western blot was performed using indicated antibody.

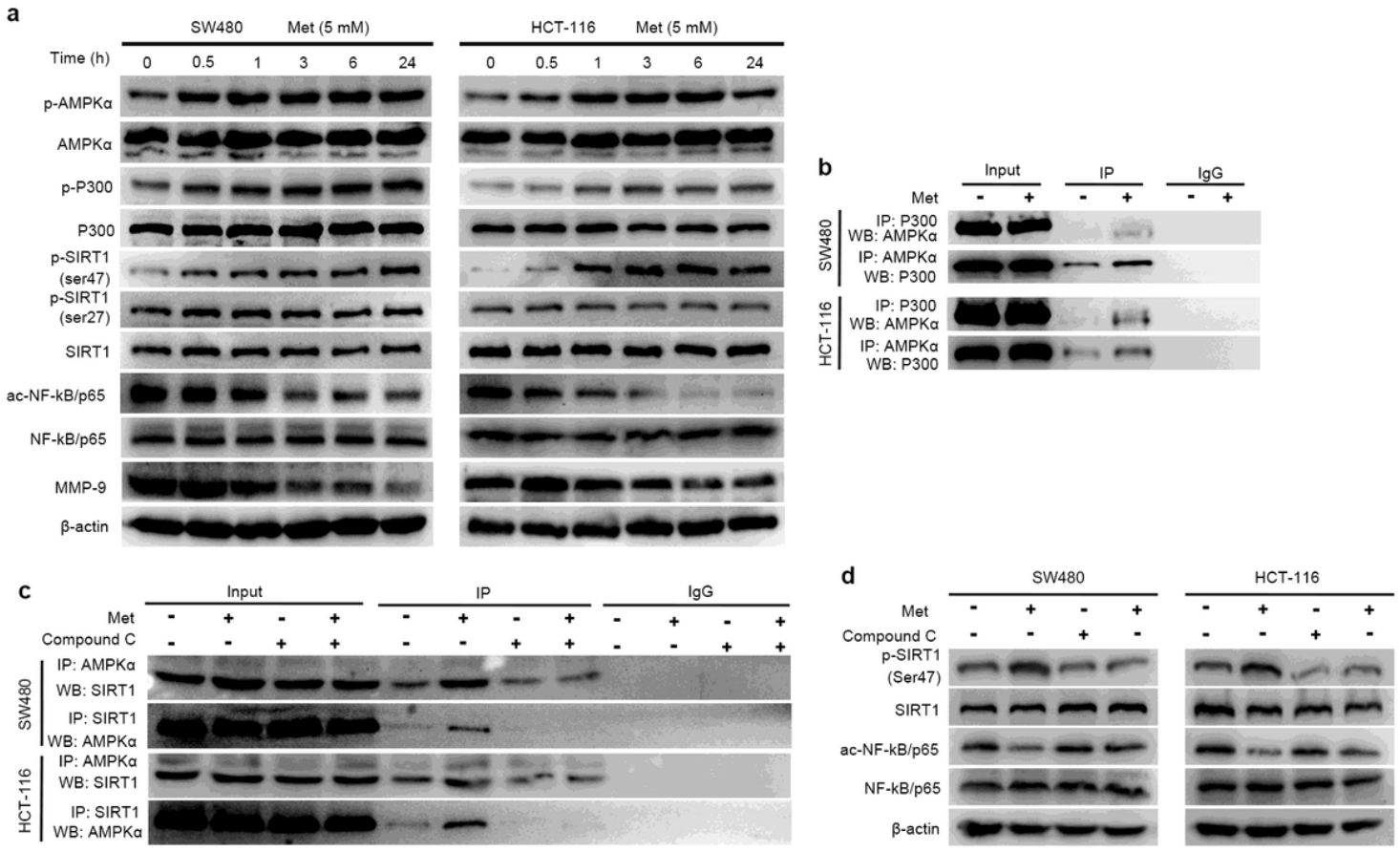

Figure 7

Metformin activates SIRT1 by inducing AMPK phosphorylation. a SW480 and HCT-116 cells were treated with the vehicle or metformin for the indicated time, and a Western blot was performed using indicated antibody. b SW480 and HCT-116 cells were treated with the vehicle or metformin (5 mM) for 24 hr. Lysates were incubated with control IgG, a rabbit anti-AMPKα antibody or a mouse anti-P300 antibody, and immunoprecipitates were analyzed by Western Blot. cSW480 and HCT-116 cells were treated with the vehicle or metformin (5 mM) in the presence or absence of Compound C (10 μM), then cells were lysed and immunoprecipitated using SIRT1 and AMPKα antibodies. The protein level was detected by Western blot using indicted antibodies. d SW480 and HCT-116 cells were treated with the vehicle or metformin (5 mM) in the presence or absence of Compound C (10 μM), and a Western blot was performed using indicated antibody.

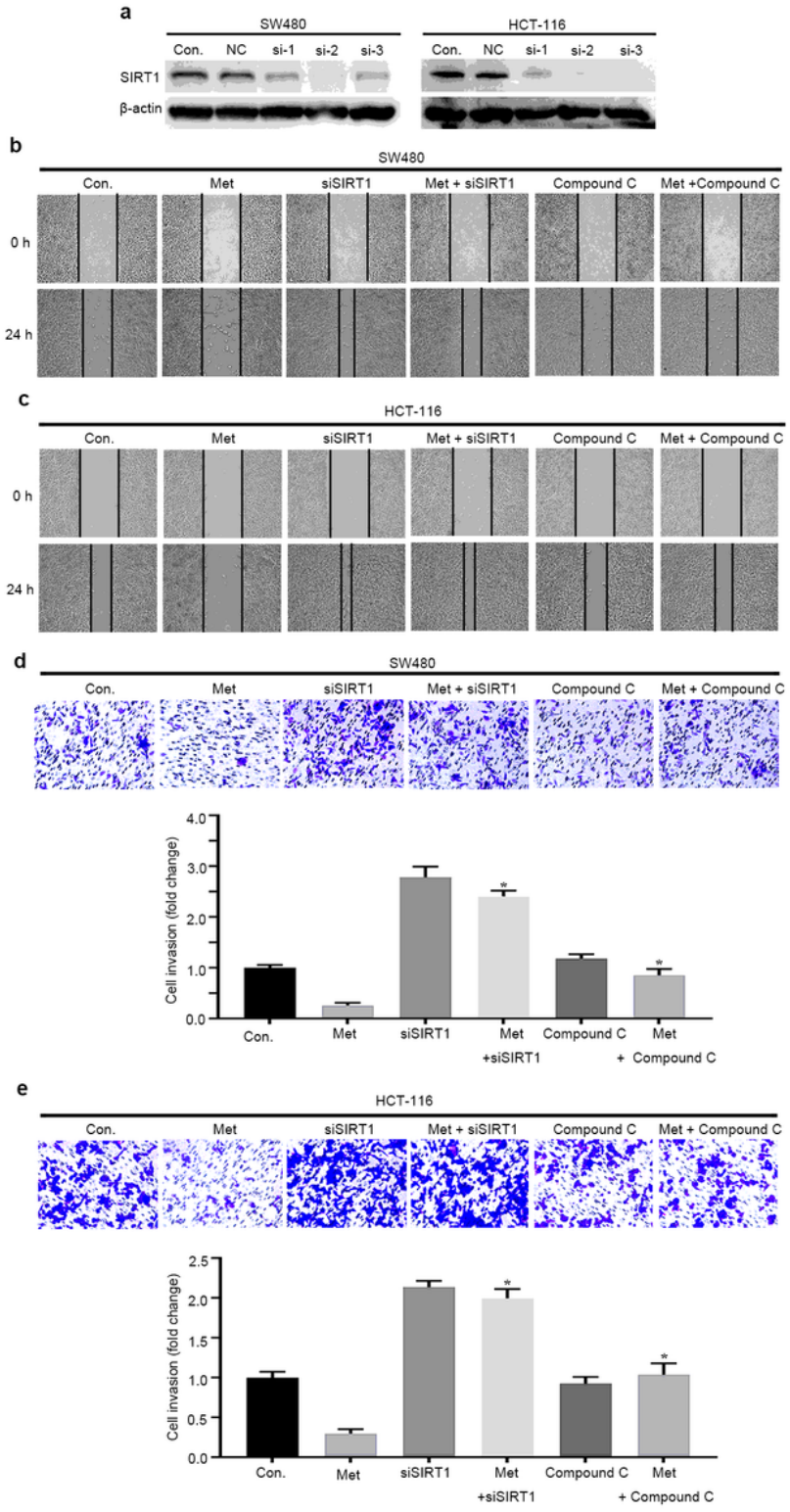

Figure 8

Inhibition of AMPK-SIRT1 complexes abolishes antimetastasis effect of metformin in CRC cells. a-d CRC cells were stimulated with metformin (5 mM) , SIRT1 siRNA, Compound C (10 μM), or the combination of two effectors. Wound healing and Transwell were used to examine the migration and invasion ability of CRC cells, respectively. *P < 0.05, compared with the Met group. *P < 0.05, compared with the Met group.

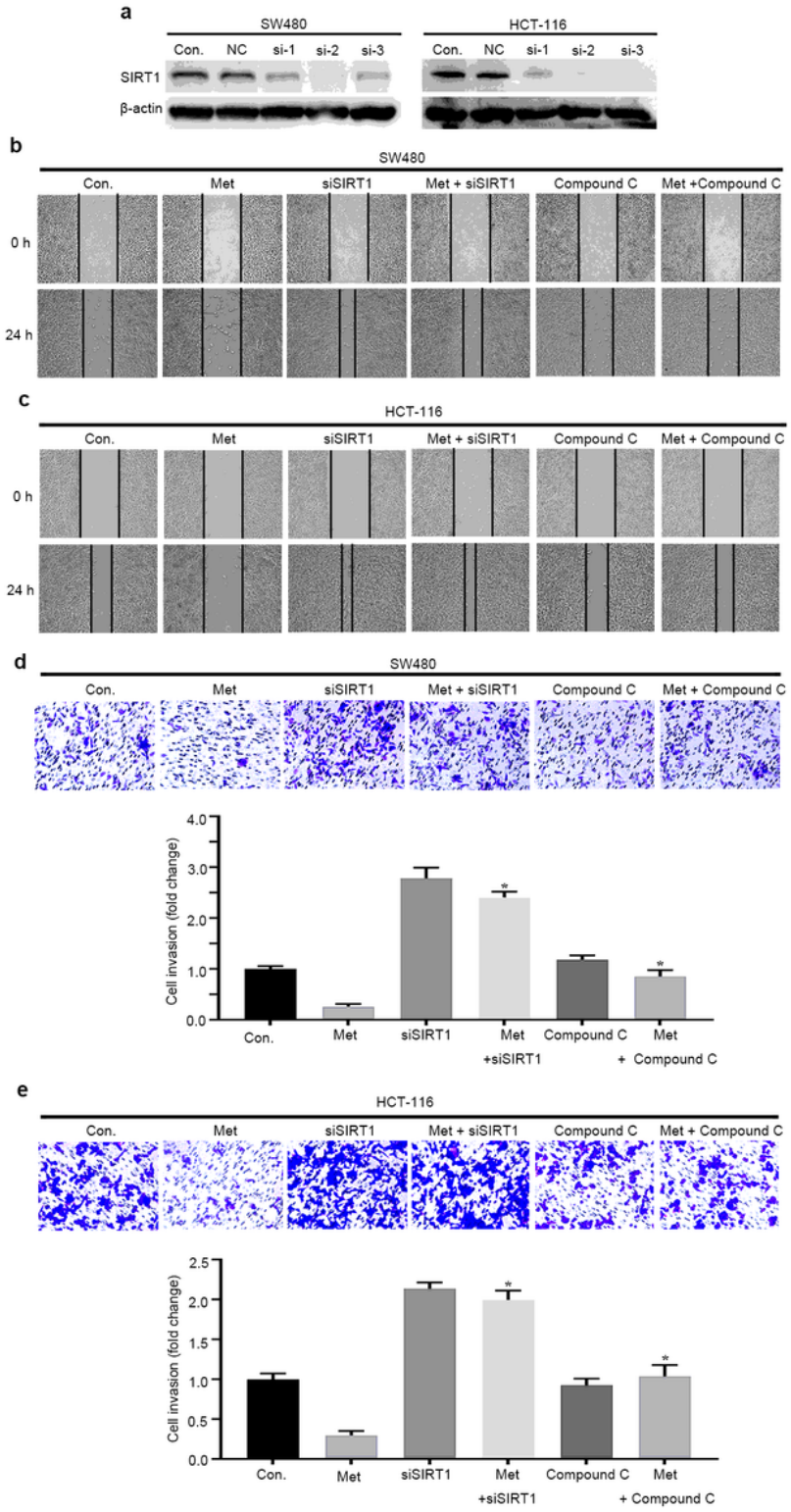

Figure 8

Inhibition of AMPK-SIRT1 complexes abolishes antimetastasis effect of metformin in CRC cells. a-d CRC cells were stimulated with metformin (5 mM) , SIRT1 siRNA, Compound C (10 μM), or the combination of two effectors. Wound healing and Transwell were used to examine the migration and invasion ability of CRC cells, respectively. *P < 0.05, compared with the Met group. *P < 0.05, compared with the Met group.

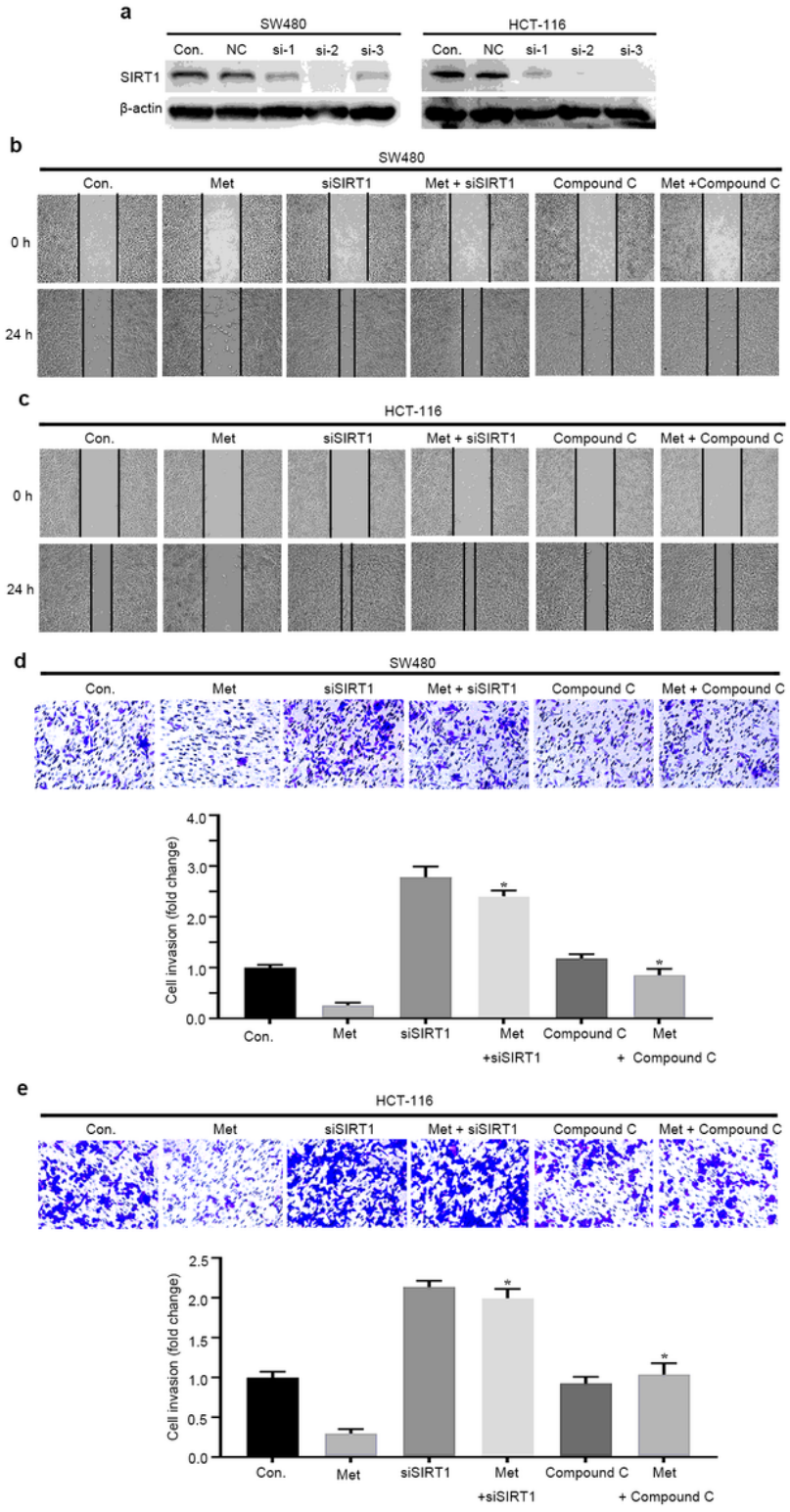

Figure 8

Inhibition of AMPK-SIRT1 complexes abolishes antimetastasis effect of metformin in CRC cells. a-d CRC cells were stimulated with metformin (5 mM) , SIRT1 siRNA, Compound C (10 μM), or the combination of two effectors. Wound healing and Transwell were used to examine the migration and invasion ability of CRC cells, respectively. *P < 0.05, compared with the Met group. *P < 0.05, compared with the Met group.

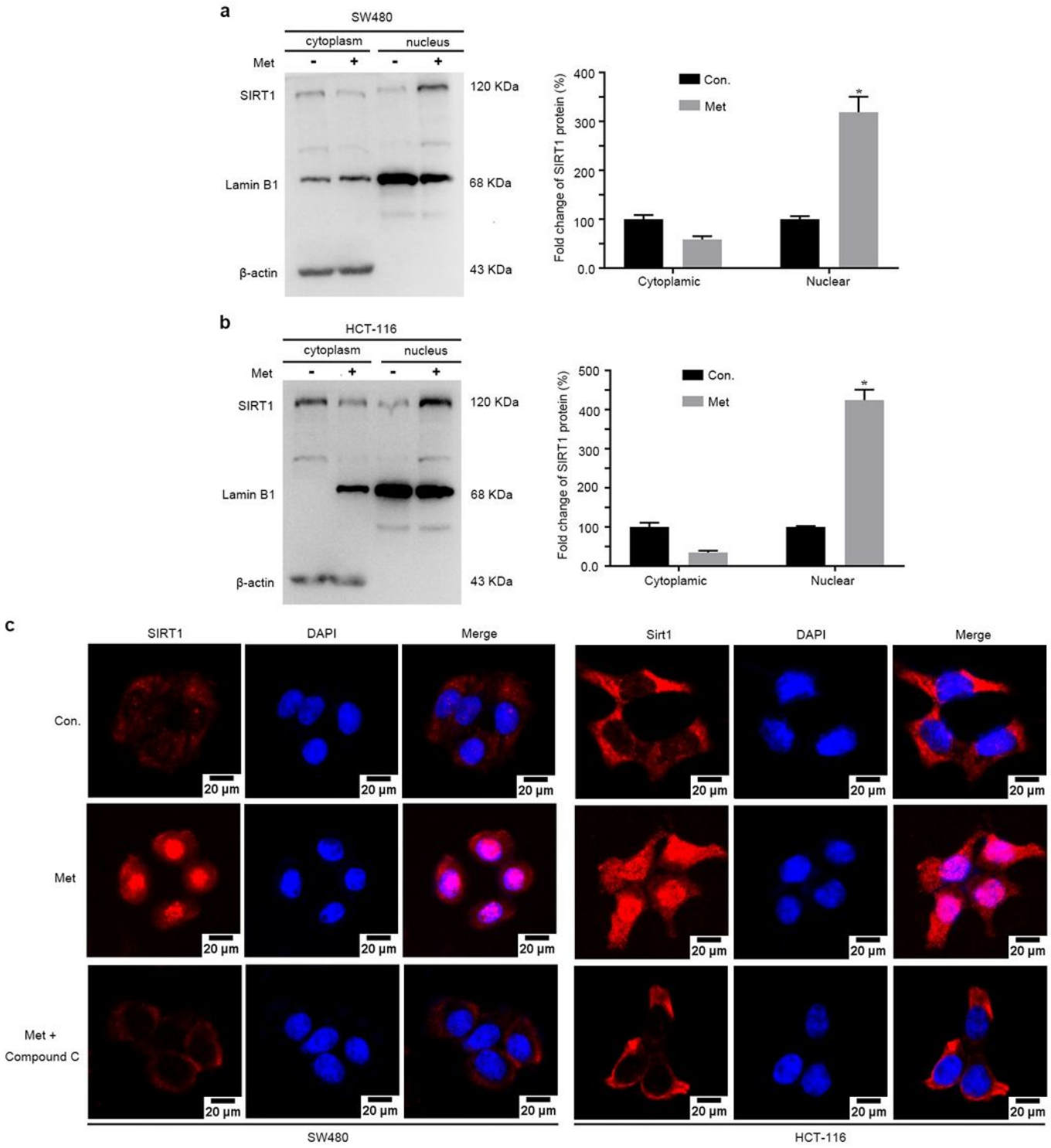

Figure 9

Metformin induces SIRT1 translocation to the cell nucleus. a and b SW480 and HCT-116 cells were treated with the vehicle or metformin (5 mM) for 24 hr. Cytoplasmic and nuclear extracts were analyzed by Western Blot using indicated antibodies. c SW480 and HCT-116 cells were treated with metformin (0, 5 mM) in the presence or absence of Compound C (10 μM). The subcellular location of SIRT1 in CRC cells

were detected by immunofluorescence staining using specific antibody, and photographed by a fluorescence microscope. *P < 0.05, compared with the control group.

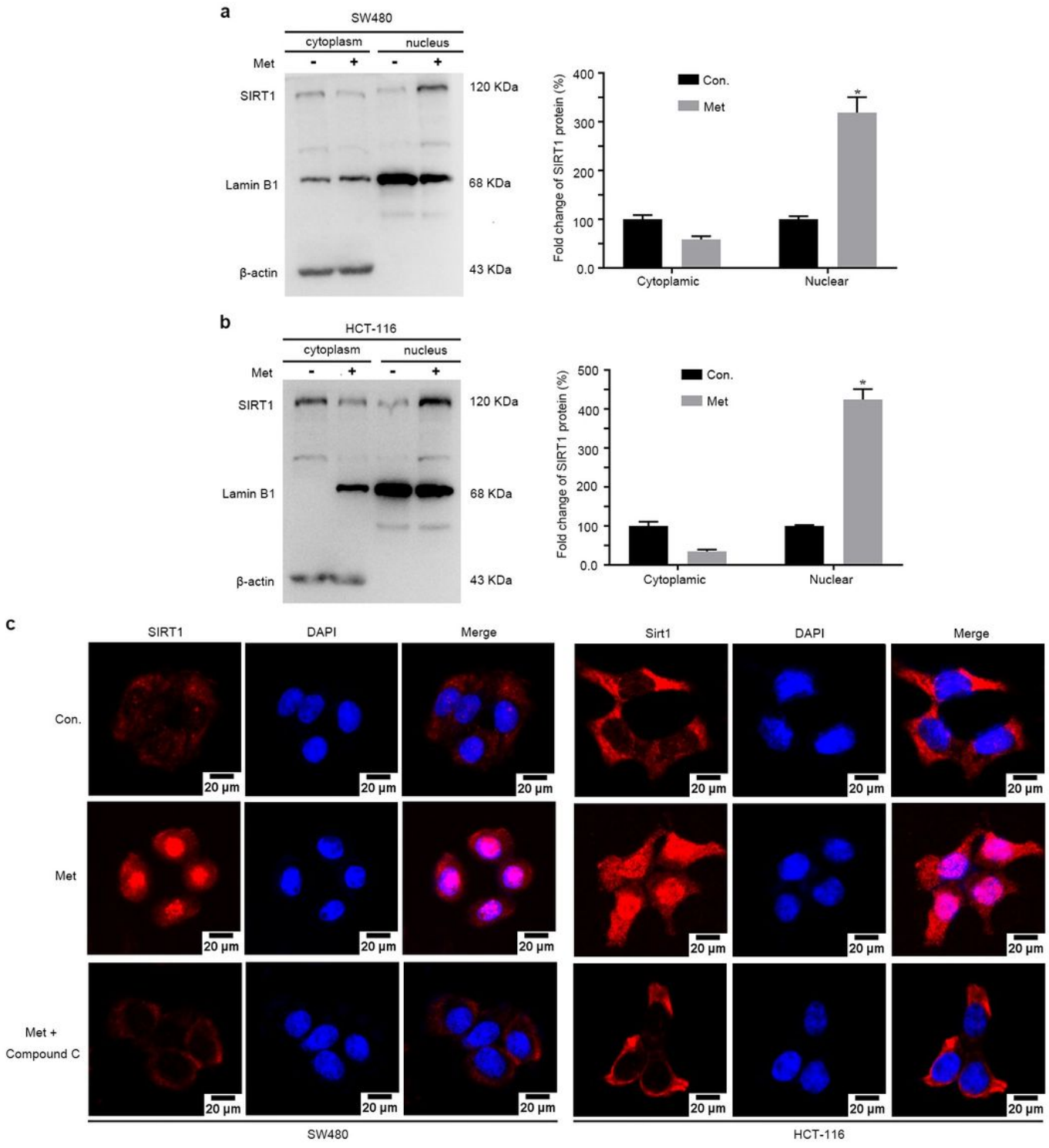

Figure 9

Metformin induces SIRT1 translocation to the cell nucleus. a and b SW480 and HCT-116 cells were treated with the vehicle or metformin (5 mM) for 24 hr. Cytoplasmic and nuclear extracts were analyzed by Western Blot using indicated antibodies. c SW480 and HCT-116 cells were treated with metformin (0, 5

mM) in the presence or absence of Compound C (10 μM). The subcellular location of SIRT1 in CRC cells were detected by immunofluorescence staining using specific antibody, and photographed by a fluorescence microscope. *P < 0.05, compared with the control group.

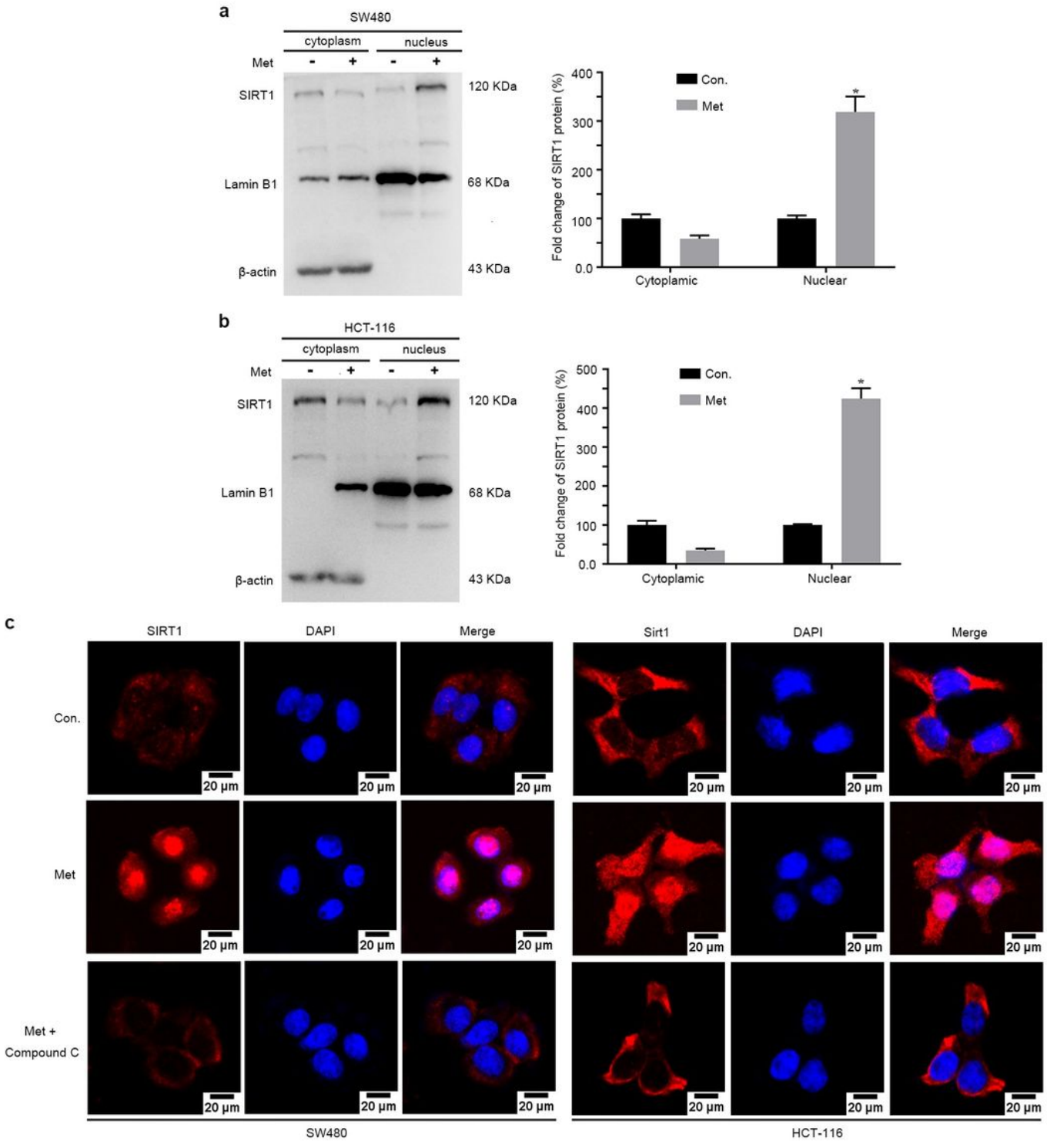

Figure 9

Metformin induces SIRT1 translocation to the cell nucleus. a and b SW480 and HCT-116 cells were treated with the vehicle or metformin (5 mM) for 24 hr. Cytoplasmic and nuclear extracts were analyzed

by Western Blot using indicated antibodies. c SW480 and HCT-116 cells were treated with metformin (0, 5 mM) in the presence or absence of Compound C (10 μM). The subcellular location of SIRT1 in CRC cells were detected by immunofluorescence staining using specific antibody, and photographed by a fluorescence microscope. *P < 0.05, compared with the control group.

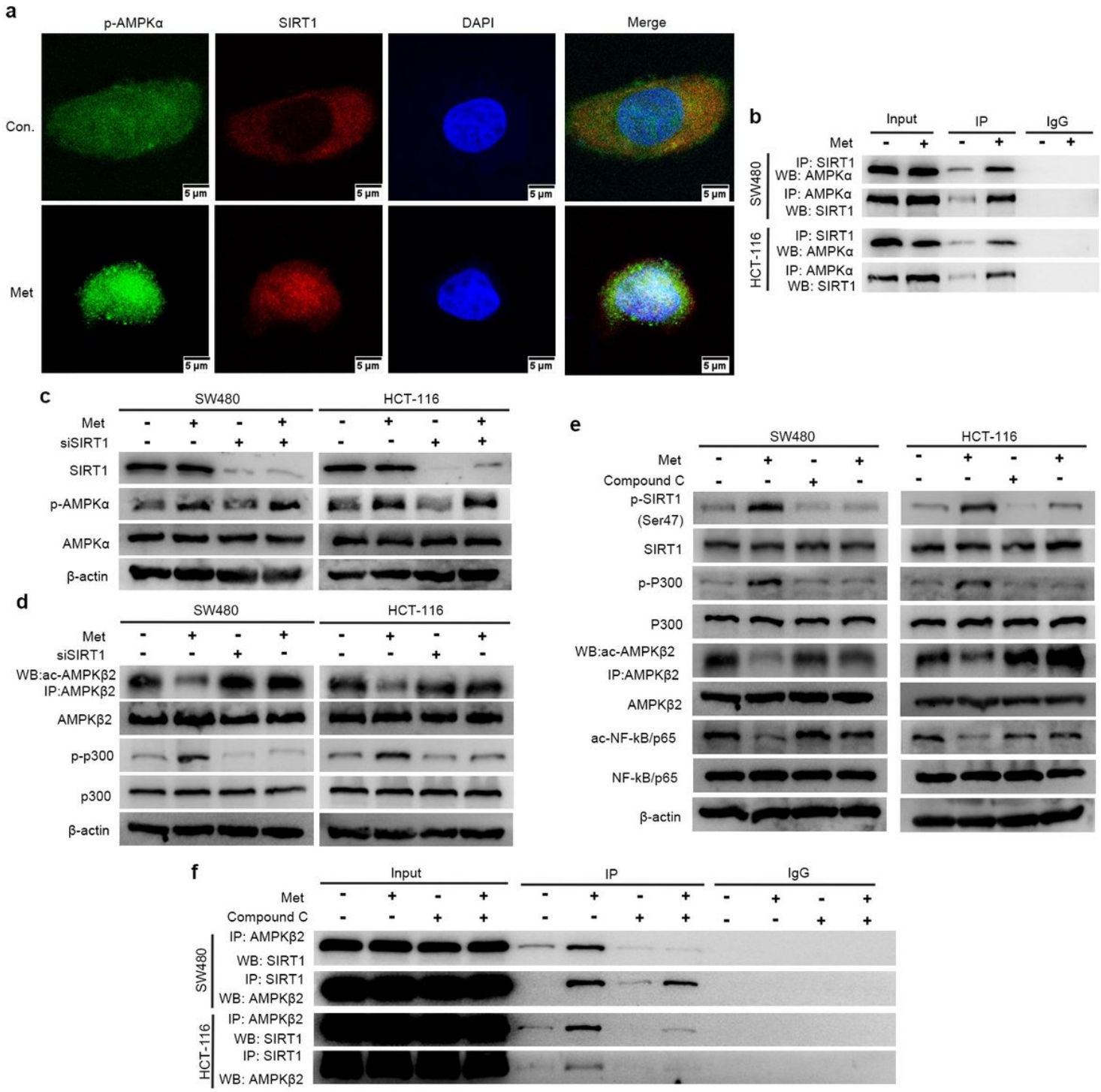

Figure 10

Phosphorylated AMPKα enhance the activity of SIRT1, and activated SIRT1 boosts the catalytic effect of AMPKα by the deacetylation of AMPKβ2 in return. a SW480 was treated with the vehicle or metformin (5

mM) for 24 hr, the expression of p-AMPK and SIRT1 were detected by immunofluorescence staining, and photographed by confocal microscopy. b and c SW480 and HCT-116 cells were transfected with a control siRNA or SIRT1 siRNA for 24 hours, the vehicle or metformin (5 mM) were added for the last 24 hr. The SIRT1, AMPKα and p-AMPKα protein levels were detected by Western blot. Lysates were also incubated with control IgG, a rabbit anti-AMPKβ2 antibody, and immunoprecipitates were analyzed by Western Blot. d and e SW480 and HCT-116 cells were treated with the vehicle or metformin (5 mM) in the presence or absence of Compound C (10 μM), then cells were lysed and immunoprecipitated using SIRT1 and AMPKβ2 antibodies. The protein level was detected by Western blot.

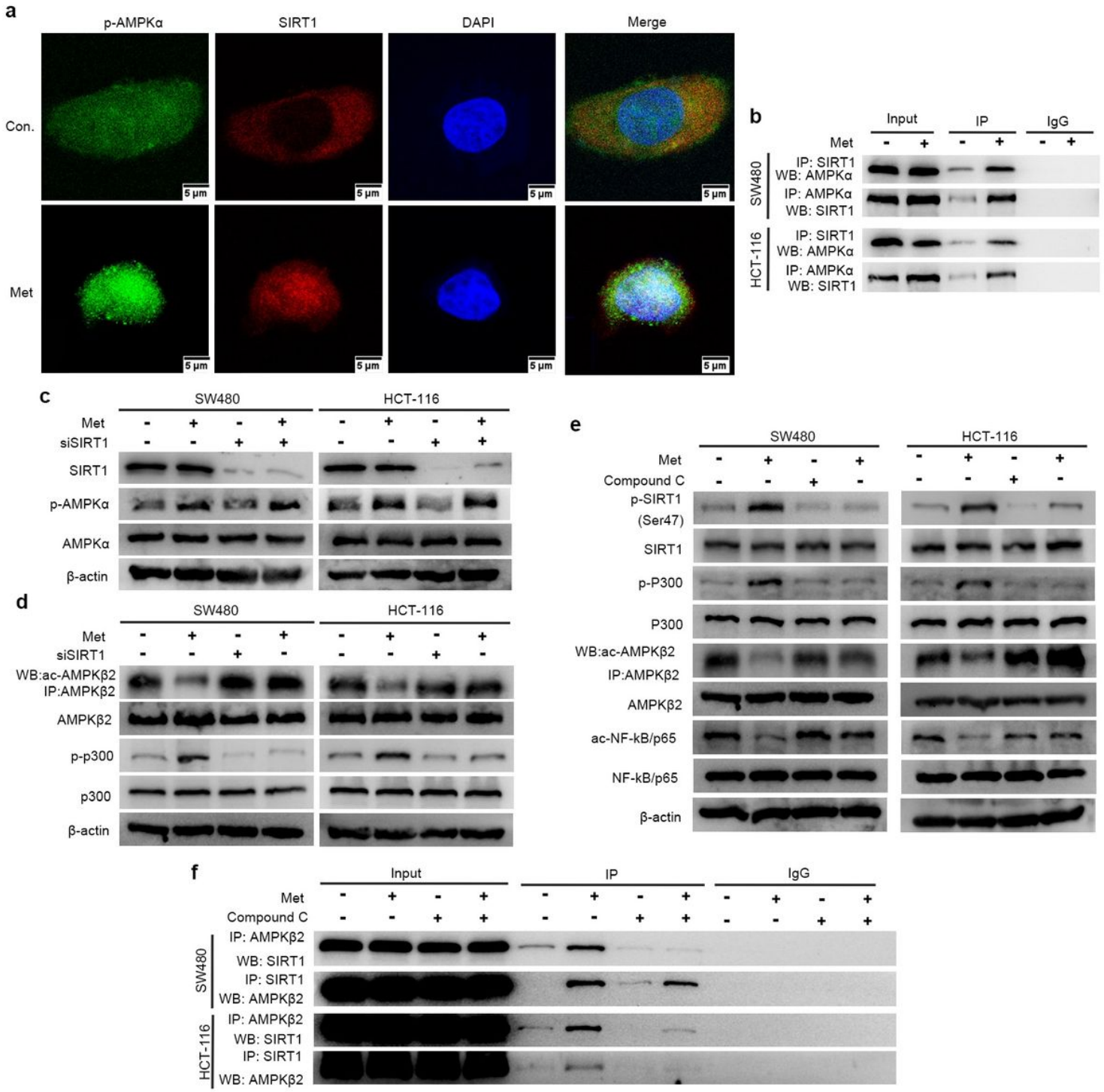

Figure 10

Phosphorylated AMPKα enhance the activity of SIRT1, and activated SIRT1 boosts the catalytic effect of AMPKα by the deacetylation of AMPKβ2 in return. a SW480 was treated with the vehicle or metformin (5 mM) for 24 hr, the expression of p-AMPK and SIRT1 were detected by immunofluorescence staining, and photographed by confocal microscopy. b and c SW480 and HCT-116 cells were transfected with a control siRNA or SIRT1 siRNA for 24 hours, the vehicle or metformin (5 mM) were added for the last 24 hr. The SIRT1, AMPKα and p-AMPKα protein levels were detected by Western blot. Lysates were also incubated with control IgG, a rabbit anti-AMPKβ2 antibody, and immunoprecipitates were analyzed by Western Blot. d and e SW480 and HCT-116 cells were treated with the vehicle or metformin (5 mM) in the presence or absence of Compound C (10 μM), then cells were lysed and immunoprecipitated using SIRT1 and AMPKβ2 antibodies. The protein level was detected by Western blot.

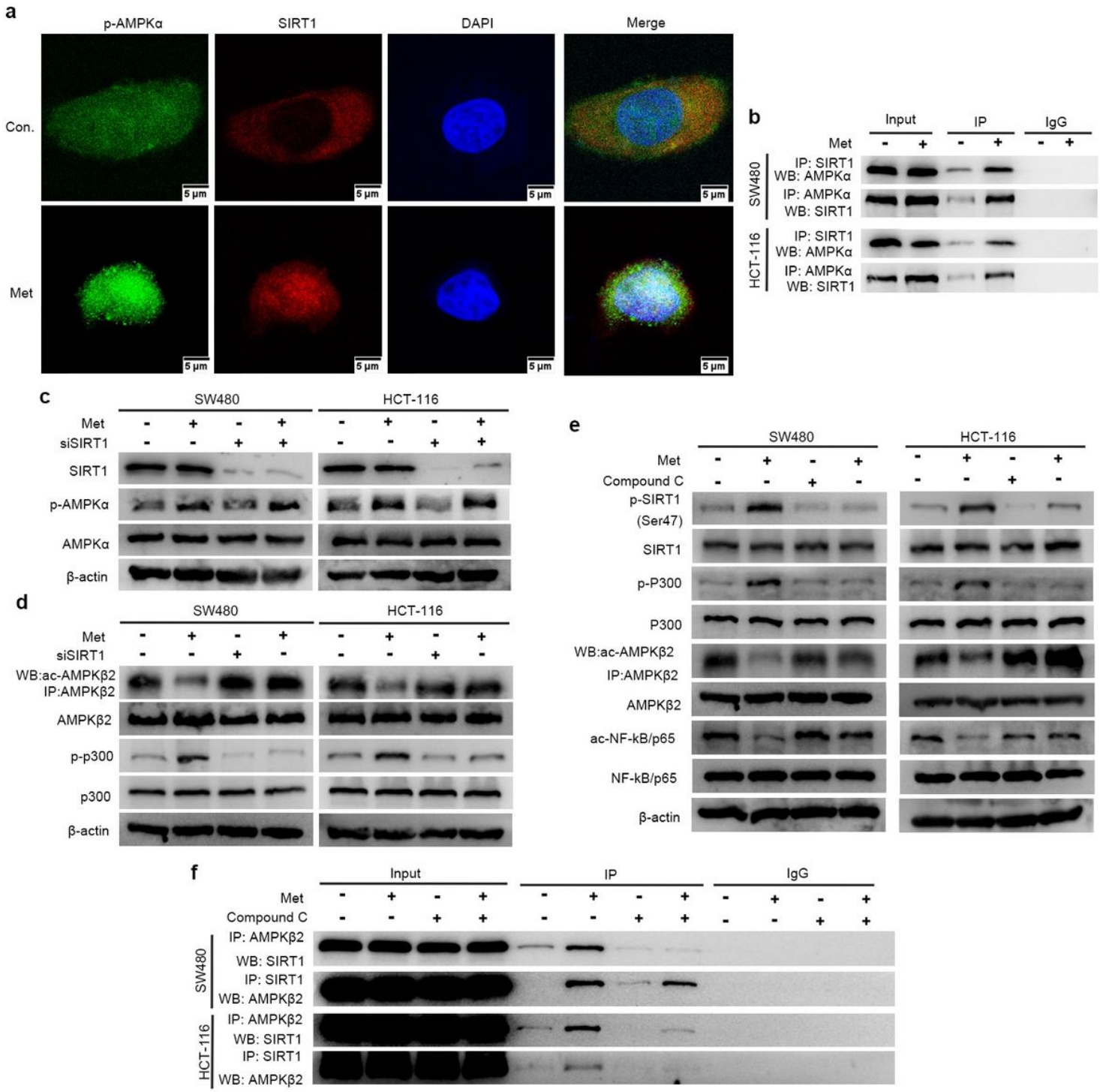

Figure 10

Phosphorylated AMPKα enhance the activity of SIRT1, and activated SIRT1 boosts the catalytic effect of AMPKα by the deacetylation of AMPKβ2 in return. a SW480 was treated with the vehicle or metformin (5 mM) for 24 hr, the expression of p-AMPK and SIRT1 were detected by immunofluorescence staining, and photographed by confocal microscopy. b and c SW480 and HCT-116 cells were transfected with a control siRNA or SIRT1 siRNA for 24 hours, the vehicle or metformin (5 mM) were added for the last 24 hr. The SIRT1, AMPKα and p-AMPKα protein levels were detected by Western blot. Lysates were also incubated

with control IgG, a rabbit anti-AMPKβ2 antibody, and immunoprecipitates were analyzed by Western Blot. d and e SW480 and HCT-116 cells were treated with the vehicle or metformin (5 mM) in the presence or absence of Compound C (10 μM), then cells were lysed and immunoprecipitated using SIRT1 and AMPKβ2 antibodies. The protein level was detected by Western blot.

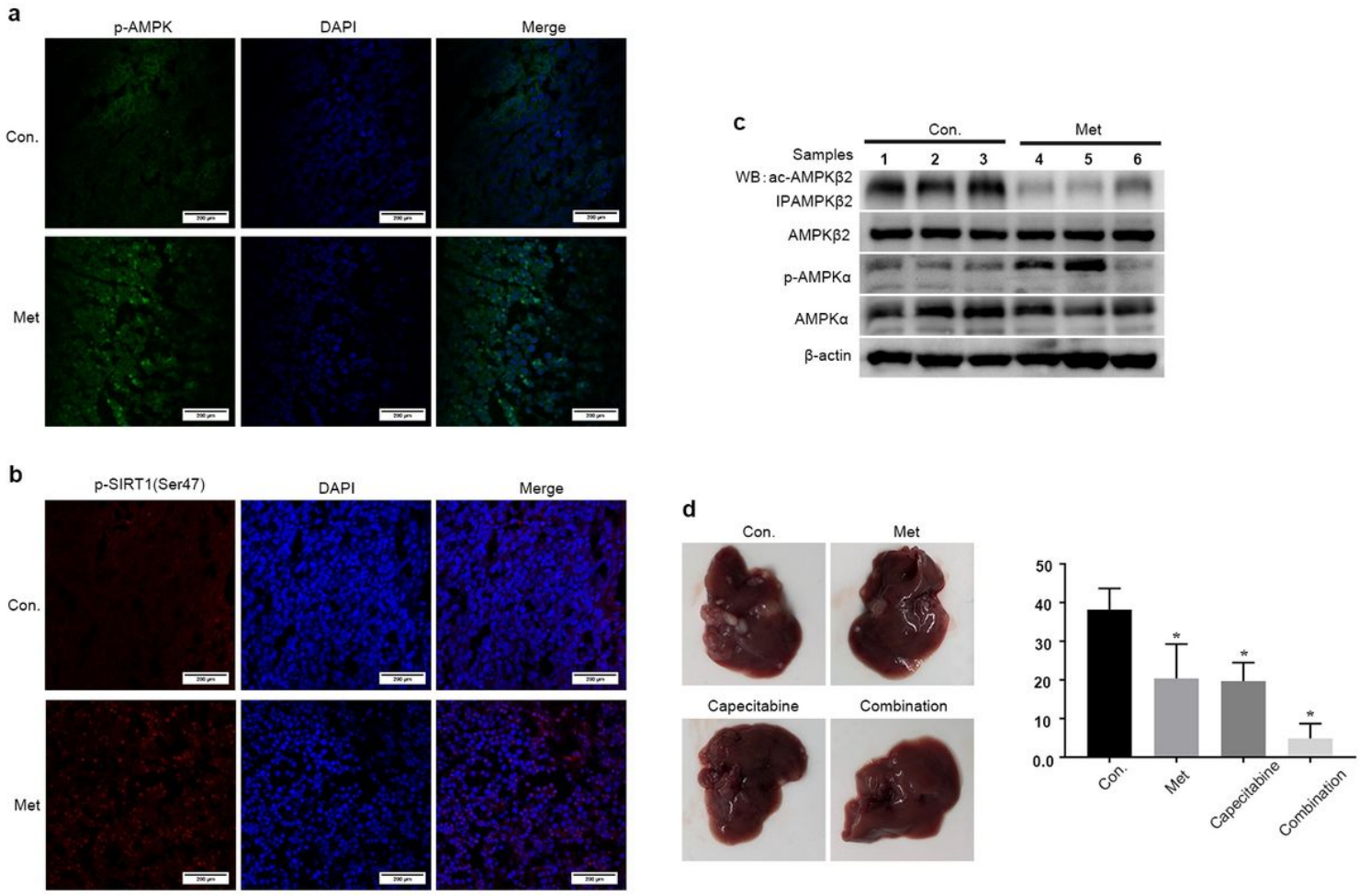

Figure 11

Metformin activates AMPK signaling pathway in vivo and enhances the ability of Capecitabine to inhibit the metastasis of CRC tumors. a and b the subcellular location of p-AMPK, p-SIRT1(Ser47). Samples came from the orthotopic tumor in spleen injection model, and Immunofluorescent staining for p-AMPK, p-SIRT1 was performed with specific antibody, photographed by confocal microscopy. c Western blot analysis of indicated proteins. d Representative images of cancer metastasis of liver were imaged after the mice were sacrificed. Left panel: Number of liver metastasis *P < 0.05, compared with the control group.

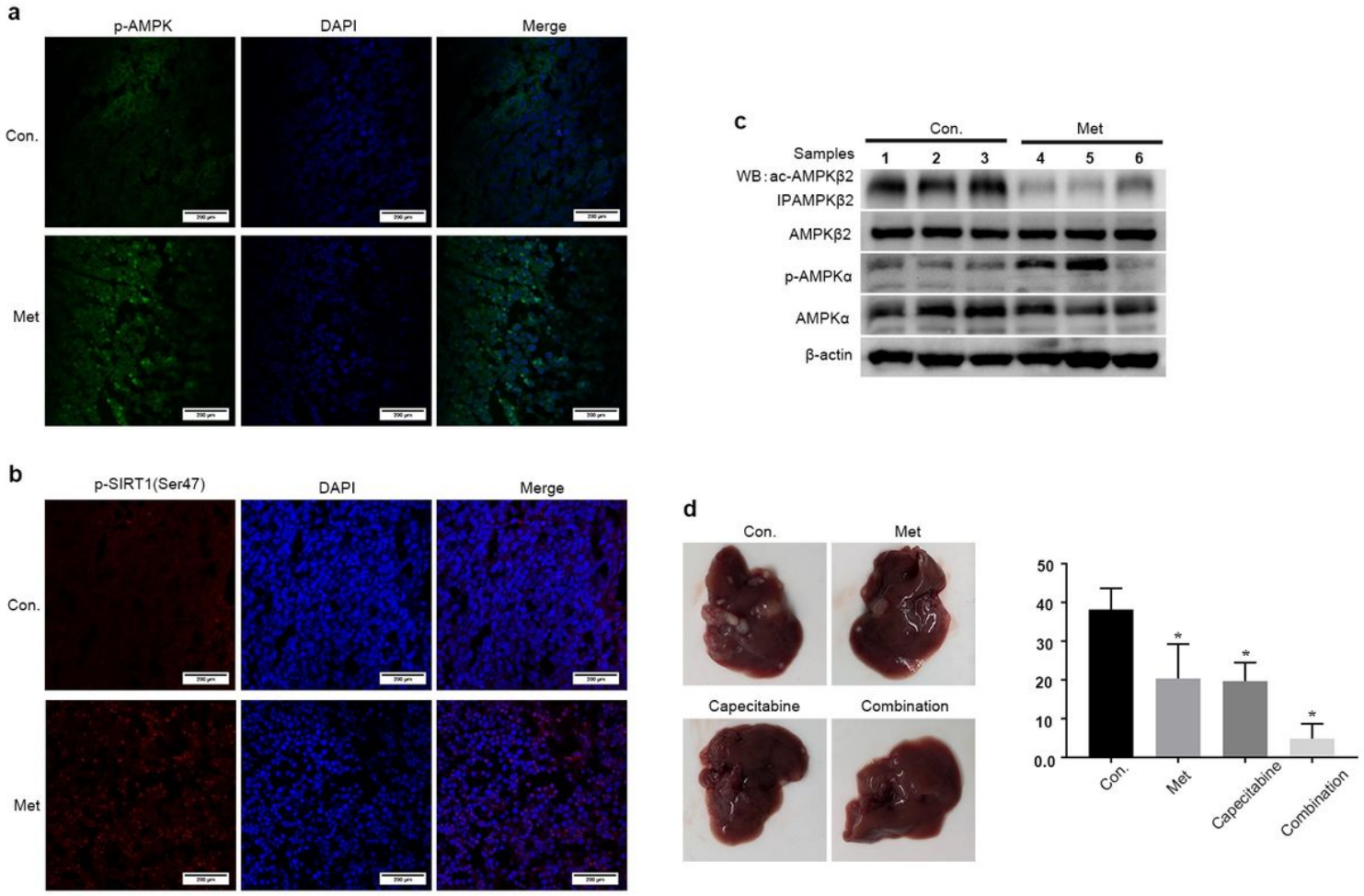

Figure 11

Metformin activates AMPK signaling pathway in vivo and enhances the ability of Capecitabine to inhibit the metastasis of CRC tumors. a and b the subcellular location of p-AMPK, p-SIRT1(Ser47). Samples came from the orthotopic tumor in spleen injection model, and Immunofluorescent staining for p-AMPK, p-SIRT1 was performed with specific antibody, photographed by confocal microscopy. c Western blot analysis of indicated proteins. d Representative images of cancer metastasis of liver were imaged after the mice were sacrificed. Left panel: Number of liver metastasis *P < 0.05, compared with the control group.

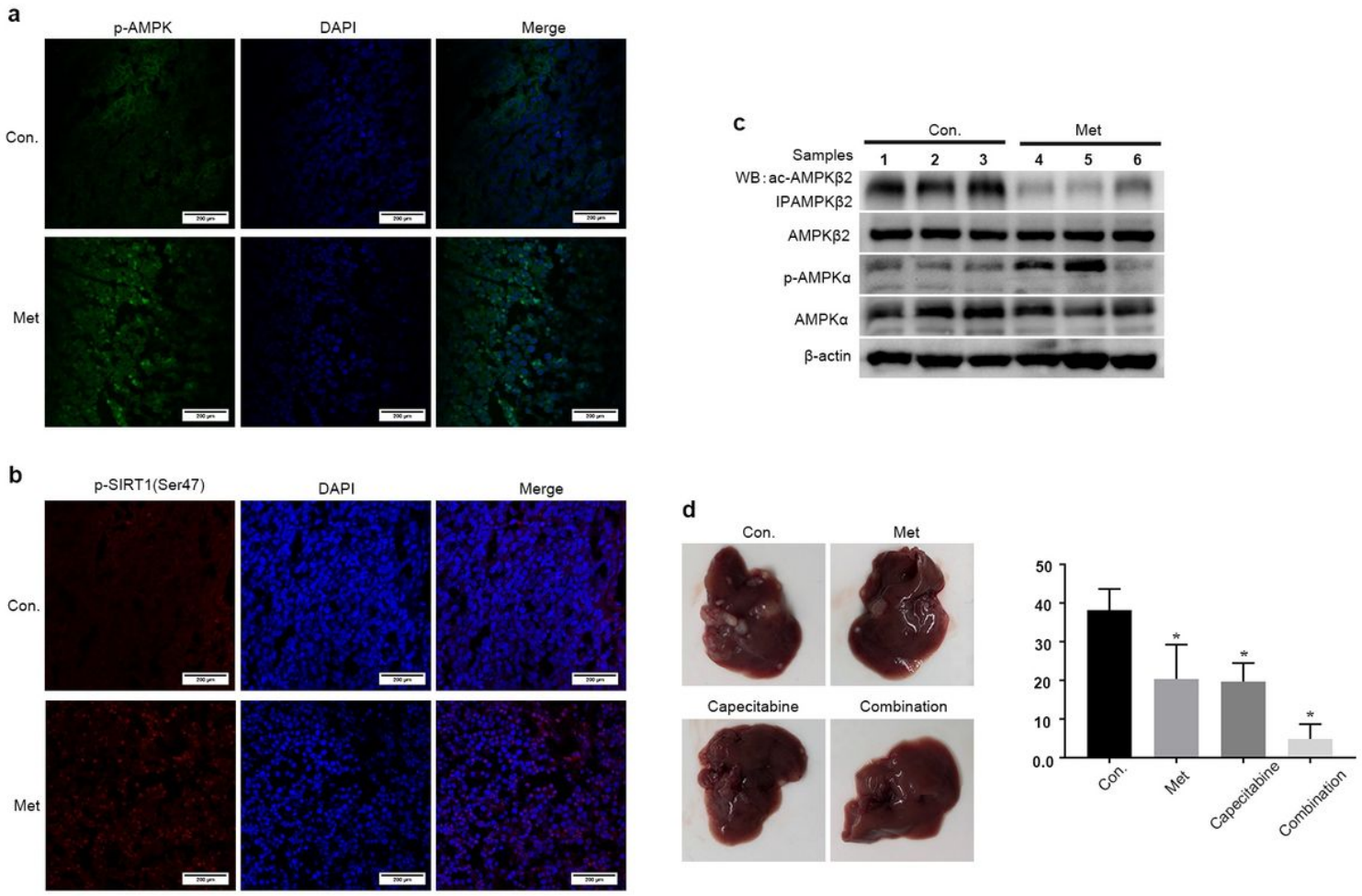

Figure 11

Metformin activates AMPK signaling pathway in vivo and enhances the ability of Capecitabine to inhibit the metastasis of CRC tumors. a and b the subcellular location of p-AMPK, p-SIRT1(Ser47). Samples came from the orthotopic tumor in spleen injection model, and Immunofluorescent staining for p-AMPK, p-SIRT1 was performed with specific antibody, photographed by confocal microscopy. c Western blot analysis of indicated proteins. d Representative images of cancer metastasis of liver were imaged after the mice were sacrificed. Left panel: Number of liver metastasis *P < 0.05, compared with the control group.

Supplementary Files

This is a list of supplementary files associated with this preprint. Click to download.

- Figs1.tif
- Figs1.tif
- Figs1.tif